NBSIR 73-331

# REFRIGERATION OF SUPERCONDUCTING ROTATING MACHINERY

Vincent D. Arp

Cryogenics Division
Institute for Basic Standards
National Bureau of Standards
Boulder, Colorado 80302

Interim Report

June 1973

Prepared for
Defense Advanced Research Projects Agency
1400 Wilson Boulevard
Arlington, Virginia 22209

NBSIR 73-331

# REFRIGERATION OF SUPERCONDUCTING ROTATING MACHINERY

Vincent D. Arp

Cryogenics Division
Institute for Basic Standards
National Bureau of Standards
Boulder, Colorado 80302

Interim Report

June 1973

Prepared for
Defense Advanced Research Projects Agency
1400 Wilson Boulevard
Arlington, Virginia 22209


U.S. DEPARTMENT OF COMMERCE, Frederick B. Dent, Secretary

NATIONAL BUREAU OF STANDARDS, Richard W. Roberts, Director

# FOREWORD

This work was performed under the sponsorship of the Defense Advanced Research Projects Agency, under Order Number 2186, beginning April 14, 1972. This report covers the 14-1/2-month period from that date to June 30, 1973. The project will terminate on December 31, 1973, and a separate report will be issued covering the last 6-month period. The ARPA program code number is 3D10, and the program monitor is Dr. E. C. Van Reuth.

CONTENTS

CONTENTS (Continued)

## LIST OF FIGURES

## LIST OF TABLES

# REFRIGERATION OF SUPERCONDUCTING ROTATING MACHINERY

Vincent D. Arp

## 1.0 Introduction

This is a report to the Advanced Research Projects Agency of the Department of Defense for work performed by the Cryogenics Division of the National Bureau of Standards from April 1972 through June 1973. Stated very briefly, the work is to assist on problems of refrigeration and system design of superconducting motors and generators. In programming this work, it has been necessary to be familiar with and responsive to related problems within DoD Laboratories, particularly the Naval Ship Research and Development Center at Annapolis, the Aero-Propulsion Laboratory at Wright Patterson AFB, and the U. S. Army Mobile Equipment Research and Development Center at Ft. Belvoir.

Section 2.0 summarizes a study of a conceivable all-high-pressure refrigeration system which might offer reduced component size and weight. Section 3.0 summarizes analytical and computational work which provides reliable basis for design of cooling channels, passages, and fluid circuits. Section 4.0 presents new forms of the equation of state for helium, arranged so as to greatly speed the calculation of helium refrigeration and flow problems. Section 5.0 summarizes survey work on refrigerator performance. Section 6.0 summarizes the relationship of this work to related work within NBS, and discusses future program plans.

A continuation of this ARPA work is funded from April through December 1973, and is oriented more than before to evaluation of liquid helium pump design and testing. This work has begun, but is not summarized here.

## 2.0 High Pressure Helium Refrigeration Cycle For Superconducting Components

### 2.1 Basic Concept

A high pressure refrigerator would offer, in principle, the possibility of reduced size because of high fluid densities throughout all the flow system. Thus, it may be useful where the refrigerator must be fitted into a small space, as in mobile applications. Assuming that the lowest pressure in the cycle is greater than the critical pressure (2.2 atmospheres, or 0.22 $MN/m^2$), the flow system would not contain any boiling liquid, and operating characteristics would not depend upon being above or below the critical temperature (5.2 Kelvin). This could be an advantage if overall system considerations should suggest optimum operation at some higher temperature, as may be feasible with $Nb_3Sn$ superconductors.

We have briefly investigated high pressure helium refrigeration cycles, since we can find no reference to previous studies. Analytical and computer techniques are used to compute cycle efficiencies and characteristics based upon realistic values of expansion engine efficiencies, heat exchanger efficiencies, and a recent NBS compilation of the real properties of fluid helium [McCarty, 1972].

### 2.2 Expansion Engine Inefficiency

The most important initial consideration for possible high pressure, helium temperature refrigerators concerns the Joule-Thomson coefficient, $\psi$. The curve labeled 0% in figure 1 is the inversion curve, along which $\psi = 0$. Above the curve, $\psi$ is negative, meaning that an isenthalpic (Joule-Thomson) expansion will cause the fluid temperature to increase. It is evident from this figure that a refrigerator cycle using a final J-T expansion from a high pressure down to about 3 atmospheres (an arbitrary pressure, a little above the critical pressure) would not be capable of

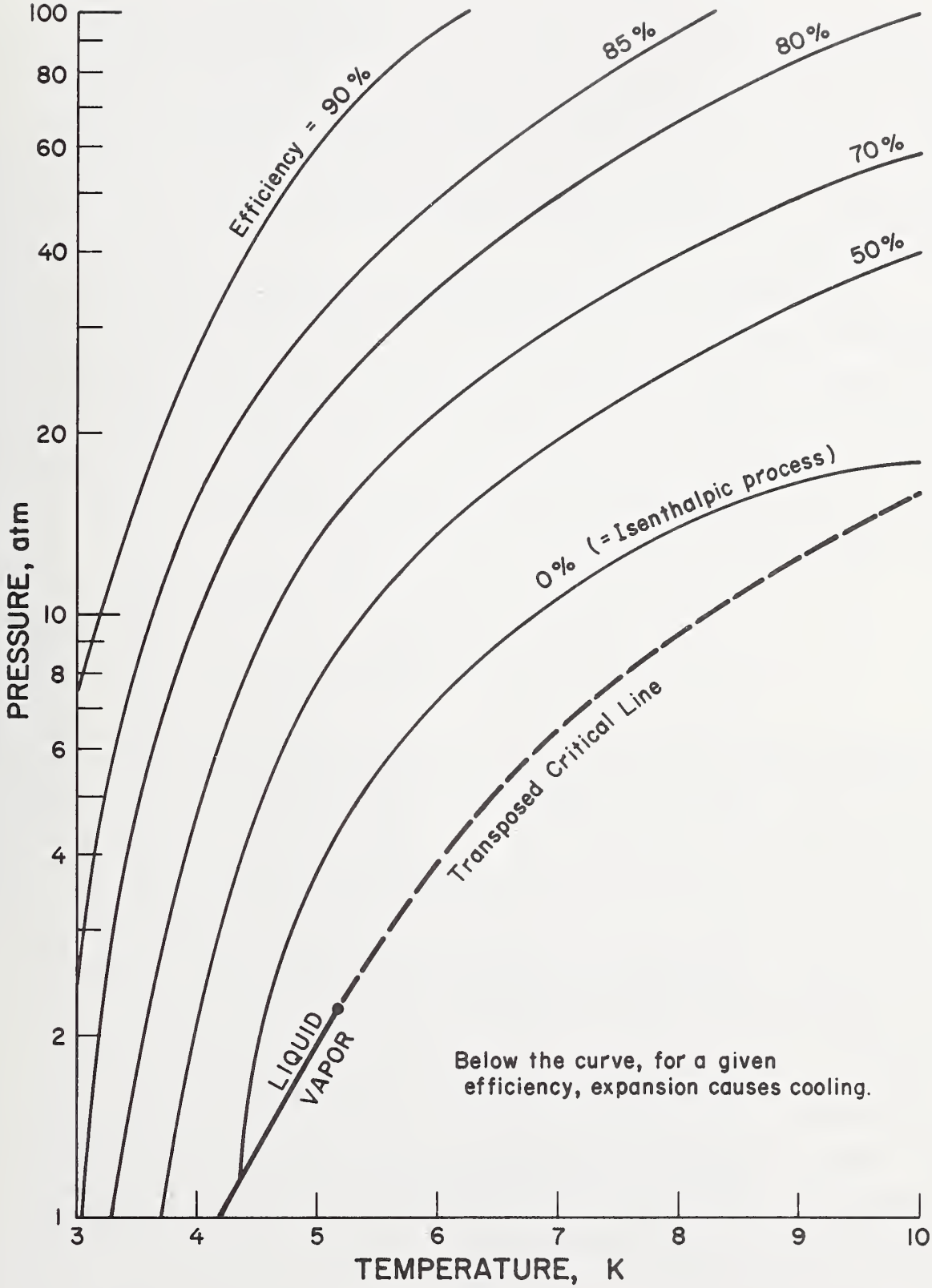


Figure 1. "Engine inversion curves" for expansion engines of stated efficiency.

refrigerating much below 5 K even at zero thermal load; in fact, subsequent calculations indicate that the minimum temperature would be closer to 10 K assuming realistic heat exchanger inefficiencies. However, if the final expansion is more nearly isentropic, as in an expansion engine, this limitation would be considerably relaxed. We consider this alternative in more detail.

Although the isentropic expansion of a real fluid always causes a temperature decrease, the inefficiency in an expansion engine, i.e., the deviation towards isenthalpic from isentropic performance, must carefully be considered in determining the temperature decrease which would be available to the refrigeration in a real system. In section 7.3 we derive the equation relating the temperature change, dT, to the pressure change, dP, through an expansion engine:

$$\frac{dT}{dP} = \psi + \frac{\epsilon}{\rho C_p} \qquad (1)$$

Expansion engine efficiencies, $\epsilon$, for helium liquefiers are typically in the range 0.60 to 0.85 [Linhart, 1973, and Strobridge, 1973]. Isentropic expansion corresponds to $\epsilon = 1.0$ and isenthalpic expansion corresponds to $\epsilon = 0$. Tables 1, 2, and 3 give values of dT/dP for engine efficiencies of 50, 70, and 85% respectively, calculated using this equation. For any given engine efficiency, then, one can define an "engine inversion curve," which is the loci of points at which $dT/dP = 0$. These are plotted in figure 1 for representative engine efficiencies. Such curves have not been presented before to our knowledge. Just as with J-T expansion, the maximum refrigeration is obtained by an expansion process in which the initial fluid state (at the engine input) lies on the engine inversion curve for the given efficiency [Dean and Mann, 1965].

Table 1. dT/dP for expansion engine of 50% efficiency as function of pressure and temperature.

dT/dP (K/ATM) FOR ENGINE AT EFFICIENCY = 50%

| PRESSURE (ATM) \ TEMPERATURE (DEGK) | 3 | 4 | 5 | 5.5 | 6 | 7 | 8 | 10 | 15 | 20 | 50 | 100 | 300 |
|---|---|---|---|---|---|---|---|---|---|---|---|---|---|
| 1 | -0.095 | 0.021 | 1.428 | 1.473 | 1.532 | 1.672 | 1.831 | 2.175 | 3.163 | 4.063 | 9.993 | 19.973 | 59.964 |
| 1.5 | -0.100 | 0.006 | 1.109 | 1.112 | 1.133 | 1.203 | 1.294 | 1.505 | 2.102 | 2.73. | 6.660 | 13.306 | 39.964 |
| 2 | -0.104 | -0.006 | 0.259 | 0.925 | 0.931 | 0.967 | 1.024 | 1.169 | 1.601 | 2.063 | 4.993 | 9.973 | 29.964 |
| 2.5 | -0.107 | -0.016 | 0.160 | 0.745 | 0.797 | 0.821 | 0.860 | 0.966 | 1.300 | 1.662 | 3.993 | 7.973 | 23.964 |
| 3 | -0.110 | -0.024 | 0.113 | 0.342 | 0.665 | 0.718 | 0.748 | 0.829 | 1.099 | 1.395 | 3.327 | 6.640 | 19.964 |
| 4 | -0.116 | -0.036 | 0.063 | 0.151 | 0.335 | 0.553 | 0.595 | 0.654 | 0.846 | 1.068 | 2.493 | 4.973 | 14.964 |
| 5 | -0.120 | -0.046 | 0.035 | 0.091 | 0.181 | 0.401 | 0.481 | 0.542 | 0.692 | 0.858 | 1.993 | 3.973 | 11.964 |
| 6 | -0.124 | -0.053 | 0.016 | 0.057 | 0.116 | 0.287 | 0.385 | 0.466 | 0.587 | 0.723 | 1.660 | 3.307 | 9.964 |
| 8 | -0.131 | -0.065 | -0.008 | 0.020 | 0.055 | 0.156 | 0.248 | 0.340 | 0.452 | 0.552 | 1.243 | 2.473 | 7.464 |
| 10 | -0.137 | -0.073 | -0.023 | -0.001 | 0.024 | 0.087 | 0.162 | 0.256 | 0.366 | 0.447 | 0.993 | 1.973 | 5.964 |
| 12 | -0.141 | -0.080 | -0.034 | -0.016 | 0.005 | 0.051 | 0.108 | 0.199 | 0.304 | 0.375 | 0.826 | 1.640 | 4.964 |
| 15 | -0.148 | -0.088 | -0.045 | -0.030 | -0.014 | 0.021 | 0.060 | 0.139 | 0.238 | 0.301 | 0.659 | 1.307 | 3.964 |
| 20 | -0.156 | -0.097 | -0.058 | -0.045 | -0.033 | -0.007 | 0.019 | 0.076 | 0.166 | 0.221 | 0.492 | 0.974 | 2.964 |
| 50 | -0.174 | -0.124 | -0.085 | -0.076 | -0.068 | -0.054 | -0.042 | -0.021 | 0.026 | 0.066 | 0.166 | 0.374 | 1.165 |
| 100 | solid | -0.114 | -0.089 | -0.084 | -0.079 | -0.069 | -0.060 | -0.045 | -0.020 | 0.002 | 0.078 | 0.173 | 0.565 |

Table 2. dT/dP for expansion engine of 70% efficiency as function of pressure and temperature.

dT/DP (K/ATM) FOR ENGINE AT EFFICIENCY = 70%

| PRESSURE (ATM) \ TEMPERATURE (DEGK) | 3 | 4 | 5 | 5.5 | 6 | 7 | 8 | 10 | 15 | 20 | 50 | 100 | 300 |
|---|---|---|---|---|---|---|---|---|---|---|---|---|---|
| 1 | -0.035 | 0.060 | 1.678 | 1.785 | 1.901 | 2.144 | 2.397 | 2.921 | 4.272 | 5.644 | 13.996 | 27.982 | 83.975 |
| 1.5 | -0.039 | 0.046 | 1.221 | 1.270 | 1.337 | 1.487 | 1.647 | 1.984 | 2.871 | 3.777 | 9.329 | 18.649 | 55.975 |
| 2 | -0.043 | 0.035 | 0.271 | 1.000 | 1.050 | 1.155 | 1.270 | 1.515 | 2.170 | 2.843 | 6.996 | 13.982 | 41.975 |
| 2.5 | -0.046 | 0.026 | 0.180 | 0.765 | 0.863 | 0.952 | 1.041 | 1.232 | 1.749 | 2.283 | 5.596 | 11.182 | 33.576 |
| 3 | -0.049 | 0.019 | 0.134 | 0.352 | 0.697 | 0.814 | 0.886 | 1.042 | 1.468 | 1.909 | 4.663 | 9.316 | 27.976 |
| 4 | -0.054 | 0.008 | 0.092 | 0.174 | 0.350 | 0.601 | 0.680 | 0.801 | 1.115 | 1.441 | 3.496 | 6.982 | 20.976 |
| 5 | -0.058 | -0.000 | 0.067 | 0.118 | 0.203 | 0.430 | 0.538 | 0.650 | 0.902 | 1.160 | 2.796 | 5.582 | 16.776 |
| 6 | -0.061 | -0.007 | 0.050 | 0.087 | 0.142 | 0.309 | 0.426 | 0.544 | 0.758 | 0.972 | 2.329 | 4.649 | 13.976 |
| 8 | -0.067 | -0.017 | 0.028 | 0.053 | 0.085 | 0.175 | 0.277 | 0.396 | 0.574 | 0.735 | 1.746 | 3.482 | 10.476 |
| 10 | -0.071 | -0.025 | 0.014 | 0.034 | 0.056 | 0.114 | 0.189 | 0.298 | 0.460 | 0.591 | 1.396 | 2.782 | 8.376 |
| 12 | -0.075 | -0.030 | 0.005 | 0.021 | 0.039 | 0.081 | 0.135 | 0.234 | 0.361 | 0.495 | 1.162 | 2.316 | 6.976 |
| 15 | -0.080 | -0.037 | -0.005 | 0.007 | 0.021 | 0.052 | 0.089 | 0.176 | 0.299 | 0.394 | 0.929 | 1.849 | 5.576 |
| 20 | -0.086 | -0.045 | -0.017 | -0.006 | 0.004 | 0.026 | 0.056 | 0.105 | 0.212 | 0.291 | 0.695 | 1.383 | 4.176 |
| 50 | -0.098 | -0.066 | -0.041 | -0.035 | -0.029 | -0.018 | -0.009 | 0.009 | 0.055 | 0.094 | 0.271 | 0.543 | 1.656 |
| 100 | solid | -0.081 | -0.047 | -0.043 | -0.040 | -0.033 | -0.027 | -0.016 | 0.007 | 0.028 | 0.125 | 0.262 | 0.816 |

Table 3. dT/dP for expansion engine of 85% efficiency as function of pressure and temperature.

dT/dP (K/ATM) FOR ENGINE AT EFFICIENCY =85%

| PRESSURE (ATM) \ TEMPERATURE (DEGK) | 3 | 4 | 5 | 5.5 | 6 | 7 | 8 | 10 | 15 | 20 | 50 | 100 | 300 |
|---|---|---|---|---|---|---|---|---|---|---|---|---|---|
| 1 | 0.010 | 0.086 | 1.605 | 2.020 | 2.177 | 2.498 | 2.822 | 3.480 | 5.148 | 6.830 | 16.998 | 33.989 | 101.984 |
| 1.5 | 0.006 | 0.076 | 1.285 | 1.388 | 1.491 | 1.699 | 1.912 | 2.344 | 3.447 | 4.563 | 11.331 | 22.656 | 67.984 |
| 2 | 0.003 | 0.066 | 0.285 | 1.056 | 1.140 | 1.296 | 1.454 | 1.774 | 2.597 | 3.429 | 8.498 | 16.989 | 50.984 |
| 2.5 | 0.000 | 0.058 | 0.196 | 0.780 | 0.913 | 1.050 | 1.177 | 1.431 | 2.086 | 2.749 | 6.798 | 13.589 | 40.784 |
| 3 | -0.003 | 0.052 | 0.157 | 0.360 | 0.721 | 0.860 | 0.989 | 1.202 | 1.745 | 2.295 | 5.665 | 11.322 | 33.984 |
| 4 | -0.007 | 0.041 | 0.115 | 0.191 | 0.361 | 0.636 | 0.744 | 0.911 | 1.317 | 1.727 | 4.248 | 8.489 | 25.484 |
| 5 | -0.010 | 0.034 | 0.091 | 0.138 | 0.219 | 0.451 | 0.586 | 0.732 | 1.059 | 1.386 | 3.398 | 6.789 | 20.384 |
| 6 | -0.013 | 0.028 | 0.075 | 0.110 | 0.161 | 0.327 | 0.456 | 0.606 | 0.866 | 1.158 | 2.831 | 5.656 | 16.984 |
| 8 | -0.018 | 0.019 | 0.055 | 0.076 | 0.107 | 0.193 | 0.296 | 0.438 | 0.666 | 0.872 | 2.123 | 4.239 | 12.734 |
| 10 | -0.022 | 0.012 | 0.043 | 0.060 | 0.081 | 0.135 | 0.208 | 0.330 | 0.531 | 0.699 | 1.698 | 3.389 | 10.184 |
| 12 | -0.025 | 0.007 | 0.034 | 0.048 | 0.064 | 0.104 | 0.156 | 0.261 | 0.439 | 0.582 | 1.414 | 2.823 | 8.484 |
| 15 | -0.029 | 0.001 | 0.024 | 0.036 | 0.048 | 0.076 | 0.111 | 0.193 | 0.344 | 0.464 | 1.131 | 2.256 | 6.784 |
| 20 | -0.034 | -0.006 | 0.014 | 0.023 | 0.032 | 0.051 | 0.073 | 0.126 | 0.247 | 0.343 | 0.847 | 1.689 | 5.084 |
| 50 | -0.041 | -0.022 | -0.008 | -0.003 | 0.001 | 0.009 | 0.016 | 0.036 | 0.076 | 0.114 | 0.334 | 0.669 | 2.025 |
| 100 | solid | -0.021 | -0.015 | -0.013 | -0.011 | -0.006 | -0.002 | 0.007 | 0.026 | 0.048 | 0.166 | 0.329 | 1.005 |

Actually there is a subtlety here which slightly clouds the accuracy of applying these curves for practical systems. The engine efficiency is defined implicitly as a function of the entropy at the engine input. Equation 1, on the other hand implicitly assumes an entropy which is defined from the pressure and temperature at each increment; in effect, this means that the efficiency defined for a finite pressure drop through the engine will not be identical to the incremental efficiency which is used in defining the inversion curves. However, we have found by trial that the differences are not large, e. g. , 70% vs 74%, in practical calculations. Hence, the engine inversion curves provide a good semi-quantitative limit to the desirable operating pressure of expansion engines. In turn, this provides an absolute lower limit to the temperature attainable with a high pressure helium cycle, independent of other parameters in the cycle.

To explore this limit quantitatively, assume for the moment that enthalpy balances in the heat exchangers and other components above the expansion engine will permit a small value of $\Delta T = T_2 - T_4$ to be obtained at the low temperature end of the heat exchanger illustrated in figure 2. For our purpose, we assume $T_2 - T_4 = 0.5$ K, which is somewhere near the minimum $\Delta T$ which might be expected in a good heat exchanger. Then performing a thermodynamic balance on just the circuit between points 2 and 4, and assuming zero thermal load, the calculated minimum possible $T_3$ is shown in figure 3 as a function of the expansion engine efficiency and exhaust pressure. The calculations were not carried below three atmospheres since (1) the hoped-for advantages in size reduction disappear, and (2) two-phase effects appear (below 2. 2 atmospheres) which would have required a more elaborate computation. Considering that expansion engine efficiencies above about 80% are difficult to achieve in practice, the important conclusion from figure 2 is that the all-high-pressure cycle is not feasible for 4 K refrigeration, though it could be for 6 or 8 K

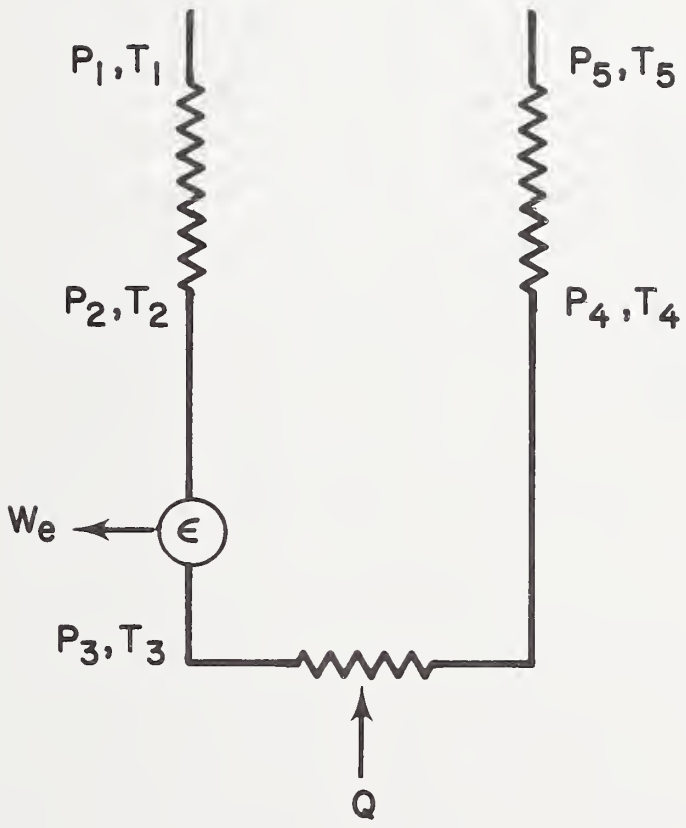


Figure 2. Low-temperature portion of the helium refrigeration cycle.

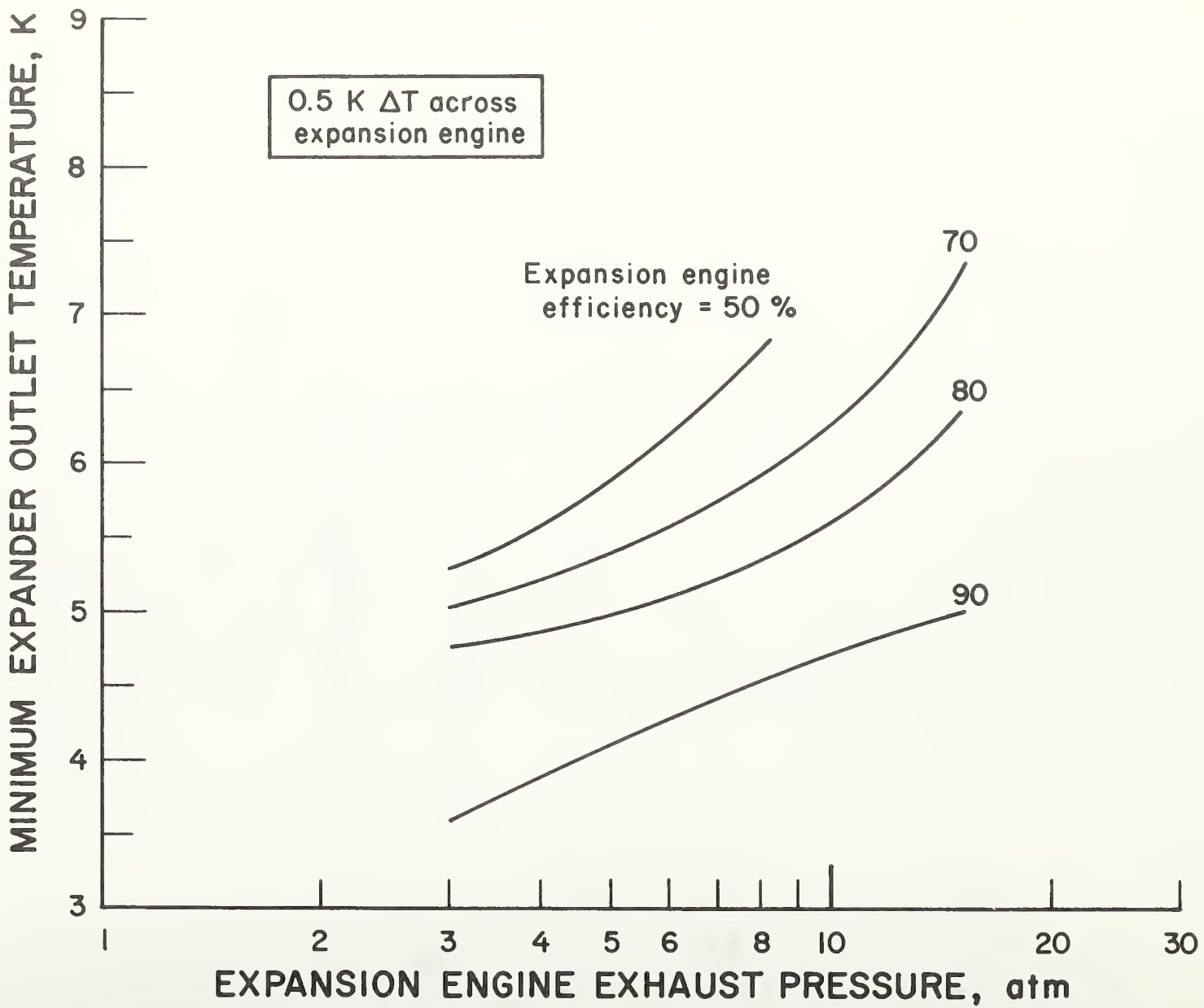


Figure 3. Minimum attainable temperature as a function of expansion engine outlet pressure, for several engine efficiencies.

B-103813

as judged by this calculation. To explore this further, we must consider the heat-exchanger and expansion engine combination as in the complete figure 2.

### 2.3 Heat Exchanger Plus Expansion Engine

Within the heat exchanger, the local temperature difference between the high and low pressure streams varies with position, due to the pressure and temperature dependence of the specific heat, as seen in figure 4. Accordingly, there is a minimum temperature difference (which must be greater than zero, from the second law of thermodynamics), somewhere within the heat exchanger. It is the minimum temperature difference which typically may be 0.5 K, but it usually does not occur at the low temperature end of the heat exchanger, as was assumed in the last section. As $T_2 - T_4$ increases from the requirements of enthalpy balance within this heat exchanger, the minimum attainable refrigeration temperatures will rise above the values determined in the previous section.

From numerical calculations, assuming $T_1$ is more than just a few degrees above $T_2$, for most conditions the minimum difference in T occurs as the top of the heat exchanger, and $T_2 - T_4$ may be as much as 3 or 4 K larger than this minimum. However, it turns out that within a restricted range of high pressures, which happen to be of interest here, viz., $P_1 \approx P_2 \approx 30$ atmospheres, $P_4 \approx P_5 \approx 5$ atmospheres, $T_4 \approx 5$ to 8 K, and $T_1 \leq 30$ K, the minimum $\Delta T$ does occur at or close to the low temperature end of the heat exchanger. For this parameter range the earlier assumption of $T_2 - T_4 = 0.5$ K would be realistic. Also it might be possible to achieve this assumed value for a wider range of conditions by adding a second expansion engine between points 1 and 4, thus unbalancing the heat exchanger mass flow rates. We have chosen not to get into a detailed mapping of these effects, since it would carry us beyond the intended scope of inquiry.

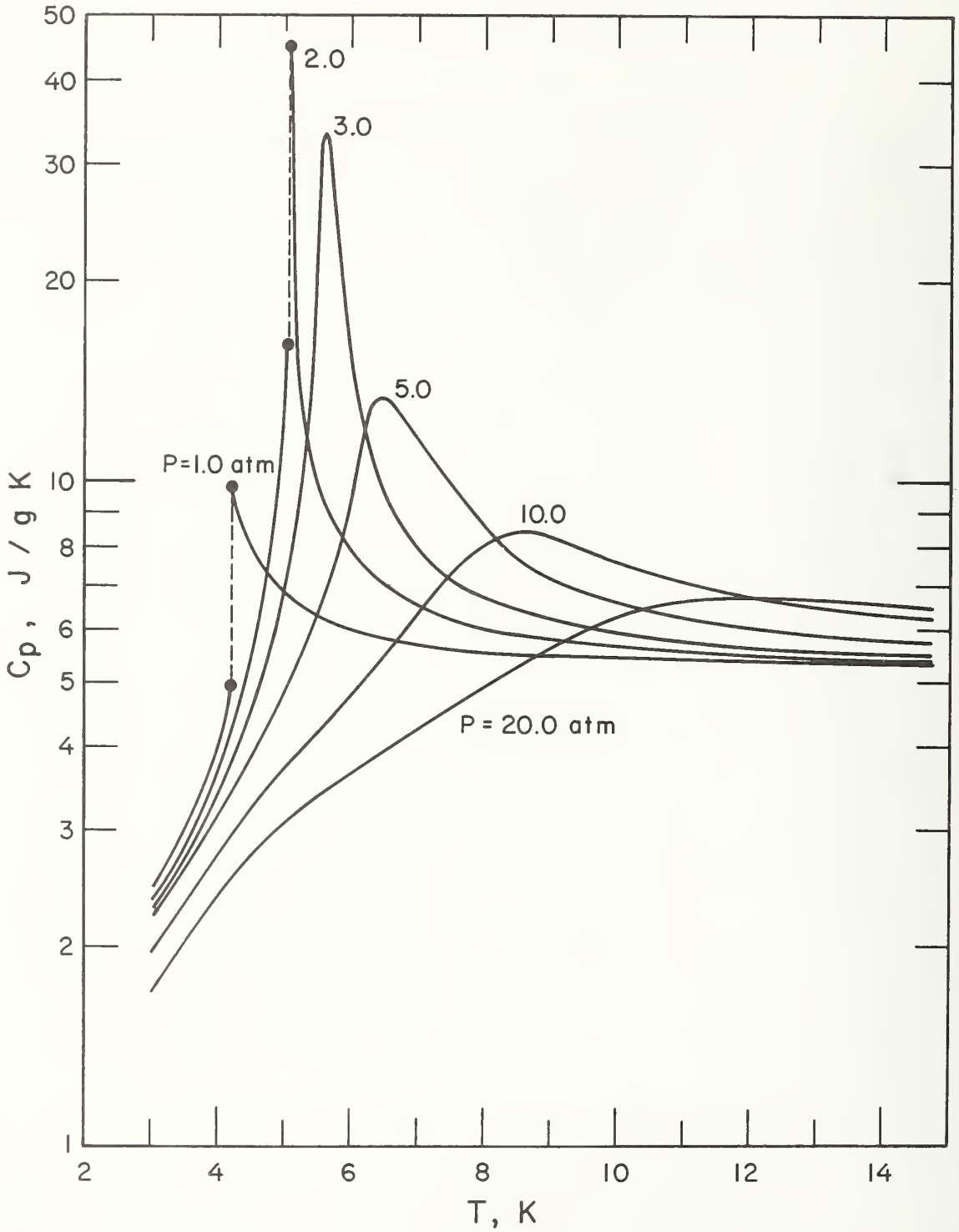


Figure 4. Specific heat as a function of temperature for several pressures.

## 2.4 Mass Flow Rates

With a non-zero thermal load, Q, the minimum attainable temperature will be higher than in figure 3 by an amount which depends on further cycle details. The ratio of the mass flow rate to the developed refrigeration is

$$\frac{\dot{m}}{Q} = \frac{1}{H_4 - H_3} \approx \frac{1}{8(T_4 - T_3)} \quad \frac{g}{W.s.}$$

where this last equality assumes refrigeration temperatures in the range 6 to 8 K and $P_3 \approx P_4$ 3 to 5 atmospheres. The magnitude of $T_4 - T_3$ will be limited by two factor (a) expansion engine inefficiencies, limiting $T_2 - T_4$, as discussed earlier, and (b) the desirability of keeping $T_4 - T_3$ small, since the load (superconductor) will experience temperatures up to $T_4$.

The corresponding value of $\dot{m}/Q$ for the conventional 4 K refrigerator with Joule-Thomson expansion to 1 atmosphere depends strongly upon the precooling temperature $T_1$, but typically can be

$$\frac{\dot{m}}{Q} \approx 0.1 \text{ to } 0.5 \quad \frac{g}{W.s.}$$

[Dean and Mann, 1965]. Without going into more detailed comparisons, beyond the scope of this work, we can say that the required mass flow rate for possible high pressure cycles would probably not be greatly different than that for the conventional cycle provided that $T_4 - T_3 \approx$ 0.3 to 1.0 K.

## 2.5 Conclusion

We have not carried out the analysis in further detail, since the cumulative factors indicate that the high pressure cycle would not be

practical at 4 K where most superconductors are designed to operate. If expansion engines of 80% efficiency or more were used, this work suggests that it could be engineered to produce useful refrigeration in a small package for temperatures above 7 or 8 K.

## 3.0 Flow of Helium in Cooling Passages

Refrigeration of superconducting components generally involves flow of helium through cooling passages, ducts, heat exchangers, etc. One direction of our work has been to set up the mechanics so that one can evaluate pressure and temperature profiles in such ducts as a function of distributed thermal loads and variable channel dimensions, etc. Because the temperature range of interest for superconducting components, roughly 3 to 8 Kelvin, spans the transposed critical line, neither the incompressible liquid nor ideal gas approximations to fluid behavior can be used in this type of analysis. Unfortunately, almost all textbooks and papers on these topics are based upon one or the other of these approximations, so that it has been necessary for us to develop the appropriate general thermohydrodynamic equations from first principles. Some of this work was reported in an earlier NBS report . For this report we have extended the earlier work considerably.

The basic goal has been to develop general analytical and computer routines for design of helium cooling systems. Copies of the computer programs have been delivered upon request to two National Laboratories, Brookhaven and Los Alamos, and we invite direct communication from other groups who may be interested in them.

### 3.1 Time-Dependent One-Dimensional Flow of a Real Fluid

We present here the equations for fluid flow in a pipe or conduit of cross section 'a' in which all radial fluid motions and radial

temperature gradients are neglected. This is a reasonable approximation for a large class of fluid flow problems in engineering design. We do allow the conduit cross section to be a slow function of position, so that we can explore the fluid changes through venturis and other smooth restrictions, but we neglect changes in elevation. The equations presented here are based on the authoritative work of Bird, Stewart, and Lightfoot (BSL) [1960].

Conservation of mass requires that

$$\frac{\partial m}{\partial z} = -a \frac{\partial \rho}{\partial t}, \tag{2}$$

and the momentum equation requires that

$$\frac{\partial P}{\partial z} = -F - \rho \frac{DU}{Dt}, \tag{3}$$

where F measures the volume force due to fluid friction, customarily written for simple one-dimensional flow in terms of an empirical friction factor f:

$$F = \frac{p}{2a} G |U| f. \tag{4}$$

Conservation of energy requires that

$$\rho \frac{DH}{Dt} = \frac{DP}{Dt} + \frac{\Lambda}{a} - \tau : \nabla U, \tag{5}$$

where $\tau$ is the stress tensor defined by BSL, and the term $\tau : \nabla U$ is the irreversible rate of conversion of mechanical energy into

internal energy of the fluid due to viscous effects. Using a dimensional argument (which I find less than wholly convincing) BSL show, in effect, that for our case of one dimensional flow in a conduit the average of this rate of conversion is just equal to the average of the volume frictional force times the fluid velocity:

$$\tau : \nabla U = FU \tag{6}$$

M. C. Jones of this laboratory has derived this equality for the case at hand using a more rigorous analytical technique (unpublished). Using this equality, and eqs (2), (3), and (4), we can finally obtain the desired expression

$$\rho \frac{D}{Dt} (H + \tfrac{1}{2} U^2) - \frac{\partial P}{\partial t} = \frac{\Lambda}{a} \tag{7}$$

which does not explicitly contain frictional effects. The steady state form of this expression was quoted in an earlier paper [Arp, 1972]. The quantity $H + 1/2\ U^2$ is known as the stagnation enthalpy.

In order to apply these equations to practical problems, one must use them in conjunction with an equation of state for the fluid, giving relationships between enthalpy, density, pressure and/or other thermodynamic properties.

### 3.2 Steady State Equations

A major milestone of our work has been to formulate and program the above equations for steady state studies without any approximations on the fluid properties, valid for all velocities up to the velocity of sound. They may also be valid for velocities greater than sound

velocity except for empirical friction factors and boundary layer heating effects, which can be neglected anyway for some problems, though we have not investigated this area. The work proceeds by performing the indicated differentiation on eq (6) and relating derivatives to the independent thermodynamic variables as in the following example

$$\frac{dH}{dz} = \frac{\partial H}{\partial P}\Big|_T \frac{dP}{dz} + \frac{\partial H}{\partial T}\Big|_P \frac{dT}{dz} \text{, etc.}$$

In the course of performing this work, certain thermodynamic identities turn out to be very useful. They are given as an addition to the nomenclature section for convenience. Note in particular the velocity

$$\omega = \sqrt{\frac{C_P}{\alpha}}$$

which might be called an expansion velocity, to distinguish it from the sound velocity c. We have found for helium that the ratio of this expansion velocity to the sound velocity is about equal to one and is remarkably independent of pressure and temperature over the whole range of fluid behavior, as can be seen from table 4. This fact can be used to obtain order-of-magnitude "feel" for the importance of various terms in the flow equations. Also for convenience, the value of $\gamma = C_p/C_v$ is given in table 5.

An earlier NBS Report, (unpublished) presented equations for pressure and temperature gradients. However, they contain a small error which becomes important as the velocity approaches sound velocity, and they assume a pipe of constant diameter. Also, because their formulation does not utilize $\omega$ or the dimensionless Mach number, the

Table 4. The ratio $\omega/C$ as a function of pressure and temperature.

"Expansion" VELOCITY FOR HELIUM/VELOCITY OF SOUND FOR HELIUM

| PRESSURE (ATM) \ TEMPERATURE (DEGK) | 3 | 4 | 5 | 5.5 | 6 | 7 | 8 | 10 | 15 | 20 | 50 | 100 | 300 |
|---|---|---|---|---|---|---|---|---|---|---|---|---|---|
| 1 | 0.885 | 0.879 | 1.203 | 1.203 | 1.203 | 1.205 | 1.207 | 1.211 | 1.216 | 1.218 | 1.223 | 1.224 | 1.225 |
| 1.5 | 0.884 | 0.870 | 1.194 | 1.192 | 1.193 | 1.195 | 1.198 | 1.204 | 1.211 | 1.215 | 1.222 | 1.223 | 1.224 |
| 2 | 0.884 | 0.862 | 0.997 | 1.181 | 1.182 | 1.186 | 1.190 | 1.197 | 1.207 | 1.212 | 1.221 | 1.223 | 1.224 |
| 2.5 | 0.883 | 0.855 | 0.954 | 1.161 | 1.170 | 1.176 | 1.182 | 1.191 | 1.202 | 1.209 | 1.220 | 1.223 | 1.224 |
| 3 | 0.883 | 0.849 | 0.930 | 1.039 | 1.150 | 1.165 | 1.173 | 1.184 | 1.196 | 1.206 | 1.219 | 1.222 | 1.224 |
| 4 | 0.883 | 0.839 | 0.900 | 0.946 | 1.042 | 1.135 | 1.153 | 1.171 | 1.189 | 1.200 | 1.217 | 1.221 | 1.224 |
| 5 | 0.884 | 0.831 | 0.880 | 0.909 | 0.960 | 1.090 | 1.128 | 1.156 | 1.180 | 1.194 | 1.215 | 1.220 | 1.224 |
| 6 | 0.884 | 0.824 | 0.865 | 0.885 | 0.920 | 1.033 | 1.098 | 1.141 | 1.171 | 1.187 | 1.213 | 1.219 | 1.223 |
| 8 | 0.886 | 0.812 | 0.843 | 0.854 | 0.876 | 0.947 | 1.028 | 1.105 | 1.154 | 1.176 | 1.209 | 1.218 | 1.223 |
| 10 | 0.886 | 0.803 | 0.827 | 0.834 | 0.849 | 0.902 | 0.969 | 1.067 | 1.137 | 1.164 | 1.205 | 1.216 | 1.223 |
| 12 | 0.887 | 0.794 | 0.815 | 0.819 | 0.831 | 0.874 | 0.929 | 1.029 | 1.120 | 1.153 | 1.201 | 1.214 | 1.222 |
| 15 | 0.886 | 0.783 | 0.800 | 0.802 | 0.812 | 0.846 | 0.893 | 0.981 | 1.096 | 1.136 | 1.195 | 1.212 | 1.222 |
| 20 | 0.878 | 0.766 | 0.782 | 0.783 | 0.790 | 0.818 | 0.853 | 0.927 | 1.063 | 1.110 | 1.186 | 1.208 | 1.220 |
| 50 | 0.703 | 0.675 | 0.723 | 0.729 | 0.737 | 0.760 | 0.783 | 0.825 | 0.923 | 0.991 | 1.134 | 1.184 | 1.214 |
| 100 | solid | 0.552 | 0.665 | 0.688 | 0.706 | 0.734 | 0.754 | 0.783 | 0.859 | 0.897 | 1.066 | 1.149 | 1.205 |

Table 5. The specific heat ratio $C_p/C_v$ as a function of pressure and temperature.

| PRESSURE (ATM) | SPECIFIC HEAT RATIO TEMPERATURE (DEGK) | | | | | | | | | | | | |
|---|---|---|---|---|---|---|---|---|---|---|---|---|---|
| | 3 | 4 | 5 | 5.5 | 6 | 7 | 8 | 10 | 15 | 20 | 50 | 100 | 300 |
| 1 | 1.233 | 1.791 | 2.137 | 1.998 | 1.919 | 1.833 | 1.787 | 1.739 | 1.698 | 1.683 | 1.668 | 1.667 | 1.667 |
| 1.5 | 1.217 | 1.700 | 2.897 | 2.342 | 2.130 | 1.945 | 1.859 | 1.779 | 1.714 | 1.691 | 1.669 | 1.667 | 1.667 |
| 2 | 1.204 | 1.633 | 5.724 | 3.128 | 2.472 | 2.086 | 1.942 | 1.820 | 1.730 | 1.700 | 1.670 | 1.667 | 1.666 |
| 2.5 | 1.192 | 1.582 | 3.233 | 6.873 | 3.112 | 2.270 | 2.038 | 1.865 | 1.747 | 1.708 | 1.671 | 1.667 | 1.666 |
| 3 | 1.182 | 1.540 | 2.624 | 7.572 | 4.493 | 2.513 | 2.150 | 1.912 | 1.764 | 1.717 | 1.672 | 1.667 | 1.666 |
| 4 | 1.164 | 1.478 | 2.144 | 3.062 | 5.714 | 3.205 | 2.425 | 2.014 | 1.798 | 1.734 | 1.674 | 1.667 | 1.666 |
| 5 | 1.150 | 1.432 | 1.926 | 2.411 | 3.397 | 3.795 | 2.735 | 2.123 | 1.833 | 1.750 | 1.676 | 1.667 | 1.666 |
| 6 | 1.138 | 1.397 | 1.796 | 2.128 | 2.667 | 3.839 | 2.981 | 2.233 | 1.867 | 1.767 | 1.677 | 1.667 | 1.666 |
| 8 | 1.119 | 1.346 | 1.643 | 1.851 | 2.128 | 2.913 | 3.131 | 2.408 | 1.931 | 1.799 | 1.681 | 1.668 | 1.666 |
| 10 | 1.105 | 1.309 | 1.552 | 1.708 | 1.897 | 2.382 | 2.839 | 2.495 | 1.985 | 1.829 | 1.684 | 1.668 | 1.665 |
| 12 | 1.094 | 1.282 | 1.490 | 1.617 | 1.763 | 2.108 | 2.492 | 2.535 | 2.028 | 1.855 | 1.688 | 1.668 | 1.665 |
| 15 | 1.082 | 1.252 | 1.426 | 1.528 | 1.638 | 1.880 | 2.152 | 2.469 | 2.067 | 1.889 | 1.692 | 1.669 | 1.665 |
| 20 | 1.069 | 1.219 | 1.358 | 1.436 | 1.517 | 1.681 | 1.858 | 2.190 | 2.082 | 1.925 | 1.700 | 1.669 | 1.664 |
| 50 | 1.035 | 1.166 | 1.218 | 1.251 | 1.283 | 1.343 | 1.405 | 1.534 | 1.796 | 1.873 | 1.731 | 1.672 | 1.660 |
| 100 | solid | 1.229 | 1.179 | 1.182 | 1.190 | 1.214 | 1.245 | 1.319 | 1.484 | 1.636 | 1.736 | 1.673 | 1.654 |

relative numerical magnitudes of the various forms are not as obvious as in the formulation below. Leaving out many tedious steps, the results of these corrected, more general calculations are:

$$(1-M^2)\frac{dP}{dz} = -\frac{p}{2a}\rho U^2(1+N^2)f_e - \frac{U}{\omega^2}\frac{\Lambda_e}{a} \tag{8}$$

$$(1-M^2)\frac{dT}{dz} = -\frac{p}{2a}\rho U^2\left(\psi+\frac{M^2}{\rho C_v}\right)f_e + \frac{\Lambda_e}{mC_p}(1-\gamma M^2) \tag{9}$$

$$(1-M^2)\frac{dH}{dz} = -\frac{p}{2a}\rho U^4\Theta f_e + \frac{\Lambda_e}{m}(1-M^2-N^2) \tag{10}$$

$$(1-M^2)\frac{d\rho}{dz} = -\frac{p}{2a}G^2\Theta f_e - \frac{\rho\Lambda_e}{m\omega^2} \tag{11}$$

$$(1-M^2)\frac{dU}{dz} = \frac{p}{2a}\rho U^3\Theta f + \frac{\Lambda}{a\rho\omega^2} - \frac{U}{a}\frac{\partial a}{\partial z} \tag{12}$$

$$\text{where } \Lambda_e \equiv \Lambda + GU^2\frac{\partial a}{\partial z}. \tag{13}$$

$$\text{and } f_e \equiv \frac{U}{|U|}f - \frac{2}{p}\frac{\partial a}{\partial z} \tag{14}$$

We can find no previous publication of these exact expressions. Especially worth noting are the effective friction factor, $f_e$, and the effective heat input per unit length, $\Lambda_e$, defined by eqs (13) and (14). Using these definitions, the correct thermodynamic and hydrodynamic profiles of flow through venturis, nozzles, etc., can be obtained by merely substituting these quantities for the usual f and $\Lambda$ appearing in conventional one-dimension equations presented here or elsewhere. We must point out, however, that since the above equations neglect energies and momenta perpendicular to the channel direction, such substitution can be accurate only for slow channel variations, i.e., only when

$$\frac{p}{4a}\frac{\partial a}{\partial z} \ll 1 .$$

It is an easy illustrative exercise to derive Bernoulli's equation

$$P_2 - P_1 + \tfrac{1}{2}\rho(U_2^2 - U_1^2) = 0$$

from eq (8) by putting f = 0, assuming $\rho$ = constant, approximating $1-M^2 \approx 1$, and integrating between two fixed flow cross sections.

Parenthetically, eq (12) is correct as written, without the subscript e on f and $\Lambda$.

The factor $1 - M^2$ which appears in these expressions deserves separate attention. It gives rise to infinite gradients at Mach 1, corresponding to a shock front. However, the Mach number

must be evaluated at the temperature of the moving stream, which may be significantly different than the stagnation temperature which the fluid would have if brought to rest adiabatically. From eq (9), neglecting friction ($f_e = 0$) and/or when the term $(\psi + M^2/\rho C_v)$ equals zero, it can be seen that when M is greater than $1/\sqrt{\gamma}$, adding thermal energy to the moving stream causes a decrease in its stream temperature, and vice versa, whereas the stagnation temperature always increases with added thermal energy. The divergence of the flow equations as the velocity approaches Mach 1 has also been explored by Chivers and Mitchell [1971] using an ideal gas approximation. Our result is in accord with theirs.

### 3.3 Integration of the Steady State Equations

We have developed, tested, and used computer programs which integrate these general steady-state equations along a flow channel of specified geometry, using the properties of helium obtained from McCarty's equations [1972, 1973] at every integration step. Using predictor-corrector techniques, the integration steps are internally adjusted to hold the integration accuracy within specified bounds. We give here an example to show the general versatility of the program, without detailed elaboration.

Figure 5 shows the profiles along a coolant passage of constant diameter, but with varying heat input. In this particular example, the pressure drops to the point that vapor would be developed within the flow channel about 60 meters from the inlet. Since the equations are valid only for single phase flow, the program stops at that point. The temperature difference between the helium and the heated wall is calculated using the correlation developed by Giarratano, et al. [1971].

HELIUM FLOW AND HEAT TRANSFER
MASS FLOW RATE = 8.000 GM/SEC
MINIMUM INTEGRATION ACCURACY = 0.00500

ASTERISKS INDICATE QUANTITIES NOT CALCULATED

| Z METERS | DIAM CM | DQ/DZ WATT/M | P ATMOS | T KELVIN | RHO GM/CM3 | TSTAG-T KELVIN | VELOC. M/S | RE NUMBER | MACH NUMBER | DEL T KELVIN | DS(DT) J/GM K | DS(F) J/GM K | S J/GM K | HSTAG J/GM | HERROR J/GM |
|---|---|---|---|---|---|---|---|---|---|---|---|---|---|---|---|
| 0.000 | 0.500 | 2.980 | 3.000 | 4.500 | 0.13001 | ****** | 3.134 | 584420 | 0.0157 | 0.047 | 0.000 | 0.000 | 3.478 | 11.412 | 0.000 |
| 1.250 | 0.500 | 2.963 | 2.980 | 4.601 | 0.12786 | ****** | 3.187 | 597046 | 0.0159 | 0.045 | 0.001 | 0.003 | 3.584 | 11.879 | 0.002 |
| 2.500 | 0.500 | 2.931 | 2.959 | 4.693 | 0.12567 | ****** | 3.242 | 609785 | 0.0162 | 0.043 | 0.002 | 0.007 | 3.687 | 12.344 | 0.006 |
| 3.750 | 0.500 | 2.874 | 2.938 | 4.777 | 0.12345 | ****** | 3.300 | 622594 | 0.0161 | 0.041 | 0.003 | 0.011 | 3.787 | 12.803 | 0.011 |
| 5.000 | 0.500 | 2.772 | 2.917 | 4.853 | 0.12123 | ****** | 3.361 | 635361 | 0.0190 | 0.038 | 0.004 | 0.014 | 3.884 | 13.251 | 0.018 |
| 6.250 | 0.500 | 2.601 | 2.895 | 4.920 | 0.11904 | ****** | 3.423 | 647867 | 0.0199 | 0.034 | 0.004 | 0.018 | 3.974 | 13.680 | 0.026 |
| 7.500 | 0.500 | 2.332 | 2.873 | 4.976 | 0.11697 | ****** | 3.483 | 659738 | 0.0208 | 0.029 | 0.005 | 0.022 | 4.058 | 14.076 | 0.035 |
| 8.750 | 0.500 | 1.954 | 2.851 | 5.021 | 0.11511 | ****** | 3.540 | 670469 | 0.0217 | 0.024 | 0.005 | 0.025 | 4.130 | 14.421 | 0.043 |
| 10.000 | 0.500 | 1.500 | 2.829 | 5.054 | 0.11354 | ****** | 3.588 | 679544 | 0.0225 | 0.018 | 0.005 | 0.029 | 4.189 | 14.698 | 0.051 |
| 11.250 | 0.500 | 1.046 | 2.806 | 5.076 | 0.11233 | ****** | 3.627 | 686678 | 0.0231 | 0.012 | 0.005 | 0.033 | 4.232 | 14.902 | 0.055 |
| 12.500 | 0.500 | 0.668 | 2.783 | 5.089 | 0.11145 | ****** | 3.656 | 691968 | 0.0236 | 0.008 | 0.005 | 0.037 | 4.263 | 15.036 | 0.057 |
| 13.750 | 0.500 | 0.399 | 2.760 | 5.096 | 0.11084 | ****** | 3.676 | 695807 | 0.0240 | 0.004 | 0.005 | 0.041 | 4.283 | 15.118 | 0.057 |
| 15.000 | 0.500 | 0.228 | 2.737 | 5.099 | 0.11041 | ****** | 3.690 | 698659 | 0.0242 | 0.002 | 0.005 | 0.046 | 4.296 | 15.163 | 0.055 |
| 16.250 | 0.500 | 0.126 | 2.714 | 5.099 | 0.11008 | ****** | 3.701 | 700901 | 0.0244 | 0.001 | 0.005 | 0.050 | 4.305 | 15.187 | 0.052 |
| 17.500 | 0.500 | 0.069 | 2.691 | 5.098 | 0.10982 | ****** | 3.710 | 702791 | 0.0246 | 0.001 | 0.005 | 0.054 | 4.311 | 15.198 | 0.048 |
| 18.750 | 0.500 | 0.037 | 2.668 | 5.096 | 0.10960 | ****** | 3.717 | 704485 | 0.0248 | 0.000 | 0.005 | 0.058 | 4.316 | 15.201 | 0.043 |
| 20.000 | 0.500 | 0.020 | 2.645 | 5.093 | 0.10940 | ****** | 3.724 | 706074 | 0.0249 | 0.000 | 0.005 | 0.062 | 4.320 | 15.201 | 0.038 |
| 21.250 | 0.500 | 0.011 | 2.622 | 5.091 | 0.10921 | ****** | 3.731 | 707611 | 0.0251 | 0.000 | 0.005 | 0.066 | 4.323 | 15.198 | 0.033 |
| 22.500 | 0.500 | 0.006 | 2.599 | 5.088 | 0.10902 | ****** | 3.737 | 709123 | 0.0252 | 0.000 | 0.005 | 0.071 | 4.327 | 15.194 | 0.027 |
| 23.750 | 0.500 | 0.003 | 2.576 | 5.085 | 0.10884 | ****** | 3.743 | 710625 | 0.0254 | 0.000 | 0.005 | 0.075 | 4.330 | 15.188 | 0.022 |
| 25.000 | 0.500 | 0.002 | 2.553 | 5.082 | 0.10866 | ****** | 3.750 | 712125 | 0.0255 | 0.000 | 0.005 | 0.079 | 4.333 | 15.183 | 0.016 |
| 26.250 | 0.500 | 0.001 | 2.529 | 5.078 | 0.10848 | ****** | 3.756 | 713629 | 0.0256 | 0.000 | 0.005 | 0.083 | 4.336 | 15.177 | 0.010 |
| 27.500 | 0.500 | 0.000 | 2.506 | 5.075 | 0.10830 | ****** | 3.762 | 715139 | 0.0258 | 0.000 | 0.005 | 0.088 | 4.340 | 15.171 | 0.003 |
| 28.750 | 0.500 | 0.000 | 2.483 | 5.072 | 0.10811 | ****** | 3.769 | 716654 | 0.0259 | 0.000 | 0.005 | 0.092 | 4.343 | 15.164 | -0.003 |
| 30.000 | 0.500 | 0.000 | 2.460 | 5.068 | 0.10793 | ****** | 3.775 | 718177 | 0.0261 | 0.000 | 0.005 | 0.096 | 4.346 | 15.157 | -0.010 |
| 32.500 | 0.500 | 0.000 | 2.413 | 5.061 | 0.10757 | ****** | 3.788 | 721245 | 0.0264 | 0.000 | 0.005 | 0.105 | 4.351 | 15.143 | -0.025 |
| 35.000 | 0.500 | 0.000 | 2.366 | 5.053 | 0.10721 | ****** | 3.800 | 724343 | 0.0267 | 0.000 | 0.005 | 0.114 | 4.357 | 15.127 | -0.040 |
| 40.000 | 0.500 | 0.000 | 2.272 | 5.038 | 0.10649 | ****** | 3.826 | 730623 | 0.0274 | 0.000 | 0.005 | 0.131 | 4.368 | 15.093 | -0.075 |
| 45.000 | 0.500 | 0.000 | 2.177 | 5.020 | 0.10577 | ****** | 3.852 | 737003 | 0.0280 | 0.000 | 0.005 | 0.149 | 4.378 | 15.053 | -0.115 |
| 50.000 | 0.500 | 0.000 | 2.082 | 5.002 | 0.10506 | ****** | 3.878 | 743463 | 0.0287 | 0.000 | 0.005 | 0.167 | 4.387 | 15.006 | -0.161 |
| 55.000 | 0.500 | 0.000 | 1.987 | 4.982 | 0.10437 | ****** | 3.904 | 749976 | 0.0294 | 0.000 | 0.005 | 0.186 | 4.395 | 14.953 | -0.214 |
| 60.000 | 0.500 | 0.000 | 1.890 | 4.961 | 0.10370 | ****** | 3.929 | 756505 | 0.0302 | 0.000 | 0.005 | 0.205 | 4.402 | 14.892 | -0.276 |

INTEGRATION TRIED TO CROSS PHASE BOUNDARY



Figure 5. Calculation of pressure, temperature, and irreversible entropy increase in helium flow through a heated channel.

The irreversible entropy increases due to fluid friction and due to the temperature difference at the wall, columns 12 and 13, are important for analysis of the overall system refrigeration requirement. The stagnation enthalpy (next to last column) should be constant over the last half of the pipe length where no heat is added, even though the pressure drops due to friction and the temperature drops due to $\psi$ ; however, the printout shows it to be slowly decreasing. Apparently this error, which is larger than most, is due to residual inaccuracy in the equation of state as the phase boundary near the critical point is approached, plus integration inaccuracy when the specific heat changes rapidly. The last column in the printout provides a thermodynamic consistency check, and is the difference between the integral of the heat added per unit length and the change in stagnation enthalpy over the stated length.

### 3.4 Flow Through a Venturi

One question which we have been concerned with is the measurement of helium flow in the near critical range through the use of venturis. Bernoulli's equation, as given above, is strictly true only for incompressible fluid flow through a venturi. For ideal gases, having a constant specific heat ratio $\gamma$ , charts and tables prepared under ASME auspices are commonly used to provide corrections to the simple Bernoulli expression. These corrections are typically a few percent in magnitude. We were concerned that the corrections due to real fluid properties in the near critical range might be a factor of ten larger, since compressibilities and thermal expansion coefficients can be larger than their ideal gas values by roughly this factor, as seen in section 7.3.

Figure 6 shows the profiles through an insulated venturi, with the added artificial assumption that the friction factor equals zero. From basic thermodynamics, such flow should take place at constant entropy and constant stagnation enthalpy. The program shows this to be the case, aside from very small errors, even though the pressure and temperature change is very significant in this near critical range. The residual errors are most probably due to slight inaccuracies in the equation of state in this range; the integration error is probably very small since the fluid velocity, at the exit, for example, is almost identical to the velocity at the inlet, after integration through all the venturi length. In this particular example, the calculated pressure difference of 0.991 atmospheres (between entrance and center of the venturi) is only 4.8% less than $\rho(U_2^2 - U_1^2)$, using $\rho = 0.08005$ g/cm$^3$ which is the density at the inlet. This is a comfortably small correction considering the close proximity to the critical point (2.25 atmospheres and 5.2 Kelvin) and the fact that the Mach number at the center reaches 0.53. We have performed such integrations for several fluid conditions and geometries, and concluded that the errors due to using the incompressible fluid Bernoulli equation even quite near the critical point will not be greater than about 5% for any practical flow condition through venturis. Because errors of this magnitude are not immediately important for the project at hand, we have decided not to take the time to quantify the corrections in some systematic way, e.g., the ASME ideal gas corrections. However, sometime in the future this could become part of an interesting study in accurate, real-fluid metrology.

HELIUM FLOW AND HEAT TRANSFER
MASS FLOW RATE = 40.000 GM/SEC
MINIMUM INTEGRATION ACCURACY = 0.00300

ASTERISKS INDICATE QUANTITIES NOT CALCULATED

FRICTION FACTOR SET = ZERO

| Z METERS | DIAM CM | DQ/DZ WATT/M | P ATMOS | T KELVIN | RHO GM/CM3 | TSTAG-T KELVIN | VELOC. M/S | RE NUMBER | MACH NUMBER | DEL T KELVIN | DS(DT) J/GM K | DS(F) J/GM K | S J/GM K | HSTAG J/GM | HERROR J/GM |
|---|---|---|---|---|---|---|---|---|---|---|---|---|---|---|---|
| 0.000 | 1.500 | 0.000 | 3.500 | 5.800 | 0.08005 | ****** | 25.450 | 4150416 | 0.2006 | ****** | ****** | ****** | 5.563 | 23.240 | 0.000 |
| 0.050 | 1.500 | 0.000 | 3.500 | 5.800 | 0.08004 | ****** | 25.459 | 4151190 | 0.2007 | ****** | ****** | ****** | 5.563 | 23.240 | 0.000 |
| 0.100 | 1.500 | 0.000 | 3.499 | 5.800 | 0.08004 | ****** | 25.484 | 4153319 | 0.2009 | ****** | ****** | ****** | 5.563 | 23.240 | 0.000 |
| 0.150 | 1.499 | 0.000 | 3.498 | 5.799 | 0.08003 | ****** | 25.552 | 4159084 | 0.2015 | ****** | ****** | ****** | 5.563 | 23.240 | 0.000 |
| 0.200 | 1.497 | 0.000 | 3.494 | 5.798 | 0.08001 | ****** | 25.734 | 4174616 | 0.2030 | ****** | ****** | ****** | 5.563 | 23.240 | 0.000 |
| 0.250 | 1.493 | 0.000 | 3.484 | 5.794 | 0.07994 | ****** | 26.219 | 4215733 | 0.2071 | ****** | ****** | ****** | 5.563 | 23.240 | 0.000 |
| 0.300 | 1.482 | 0.000 | 3.458 | 5.783 | 0.07977 | ****** | 27.463 | 4319969 | 0.2178 | ****** | ****** | ****** | 5.564 | 23.241 | 0.001 |
| 0.350 | 1.460 | 0.000 | 3.391 | 5.755 | 0.07934 | ****** | 30.379 | 4557946 | 0.2432 | ****** | ****** | ****** | 5.564 | 23.243 | 0.003 |
| 0.400 | 1.425 | 0.000 | 3.248 | 5.695 | 0.07840 | ****** | 35.970 | 4994740 | 0.2941 | ****** | ****** | ****** | 5.564 | 23.246 | 0.006 |
| 0.450 | 1.390 | 0.000 | 3.019 | 5.593 | 0.07680 | ****** | 43.534 | 5560927 | 0.3689 | ****** | ****** | ****** | 5.564 | 23.245 | 0.005 |
| 0.500 | 1.368 | 0.000 | 2.782 | 5.483 | 0.07483 | ****** | 50.315 | 6057319 | 0.4441 | ****** | ****** | ****** | 5.571 | 23.288 | 0.048 |
| 0.375 | 1.443 | 0.000 | 3.331 | 5.730 | 0.07854 | ****** | 32.820 | 4751430 | 0.2650 | ****** | ****** | ****** | 5.564 | 23.245 | 0.005 |
| 0.400 | 1.425 | 0.000 | 3.247 | 5.694 | 0.07837 | ****** | 35.983 | 4995965 | 0.2943 | ****** | ****** | ****** | 5.565 | 23.248 | 0.008 |
| 0.425 | 1.407 | 0.000 | 3.139 | 5.647 | 0.07761 | ****** | 39.694 | 5276189 | 0.3300 | ****** | ****** | ****** | 5.565 | 23.252 | 0.012 |
| 0.450 | 1.390 | 0.000 | 3.016 | 5.592 | 0.07672 | ****** | 43.583 | 5564685 | 0.3696 | ****** | ****** | ****** | 5.566 | 23.257 | 0.017 |
| 0.475 | 1.377 | 0.000 | 2.892 | 5.535 | 0.07578 | ****** | 47.215 | 5831359 | 0.4087 | ****** | ****** | ****** | 5.567 | 23.263 | 0.023 |
| 0.500 | 1.368 | 0.000 | 2.782 | 5.482 | 0.07491 | ****** | 50.257 | 6054217 | 0.4434 | ****** | ****** | ****** | 5.568 | 23.267 | 0.027 |
| 0.525 | 1.361 | 0.000 | 2.694 | 5.440 | 0.07420 | ****** | 52.581 | 6224838 | 0.4713 | ****** | ****** | ****** | 5.568 | 23.268 | 0.028 |
| 0.550 | 1.357 | 0.000 | 2.630 | 5.407 | 0.07367 | ****** | 54.233 | 6346674 | 0.4919 | ****** | ****** | ****** | 5.568 | 23.269 | 0.029 |
| 0.575 | 1.354 | 0.000 | 2.586 | 5.385 | 0.07330 | ****** | 55.350 | 6429297 | 0.5063 | ****** | ****** | ****** | 5.568 | 23.269 | 0.029 |
| 0.600 | 1.353 | 0.000 | 2.556 | 5.370 | 0.07305 | ****** | 56.077 | 6483264 | 0.5158 | ****** | ****** | ****** | 5.568 | 23.270 | 0.030 |
| 0.625 | 1.352 | 0.000 | 2.538 | 5.360 | 0.07289 | ****** | 56.539 | 6517582 | 0.5219 | ****** | ****** | ****** | 5.568 | 23.271 | 0.031 |
| 0.650 | 1.351 | 0.000 | 2.526 | 5.354 | 0.07278 | ****** | 56.826 | 6539004 | 0.5257 | ****** | ****** | ****** | 5.569 | 23.272 | 0.032 |
| 0.675 | 1.351 | 0.000 | 2.519 | 5.350 | 0.07272 | ****** | 57.003 | 6552199 | 0.5281 | ****** | ****** | ****** | 5.569 | 23.272 | 0.032 |
| 0.700 | 1.350 | 0.000 | 2.515 | 5.348 | 0.07268 | ****** | 57.111 | 6560234 | 0.5296 | ****** | ****** | ****** | 5.569 | 23.272 | 0.032 |
| 0.725 | 1.350 | 0.000 | 2.512 | 5.347 | 0.07266 | ****** | 57.175 | 6565047 | 0.5304 | ****** | ****** | ****** | 5.569 | 23.272 | 0.032 |
| 0.750 | 1.350 | 0.000 | 2.510 | 5.346 | 0.07265 | ****** | 57.212 | 6567820 | 0.5309 | ****** | ****** | ****** | 5.569 | 23.272 | 0.032 |
| 0.800 | 1.350 | 0.000 | 2.509 | 5.345 | 0.07264 | ****** | 57.237 | 6569684 | 0.5313 | ****** | ****** | ****** | 5.569 | 23.272 | 0.032 |
| 0.850 | 1.350 | 0.000 | 2.510 | 5.346 | 0.07265 | ****** | 57.213 | 6567833 | 0.5309 | ****** | ****** | ****** | 5.569 | 23.272 | 0.032 |
| 0.900 | 1.350 | 0.000 | 2.515 | 5.348 | 0.07268 | ****** | 57.111 | 6560222 | 0.5296 | ****** | ****** | ****** | 5.569 | 23.272 | 0.032 |
| 0.950 | 1.351 | 0.000 | 2.526 | 5.354 | 0.07279 | ****** | 56.825 | 6538908 | 0.5257 | ****** | ****** | ****** | 5.569 | 23.272 | 0.032 |
| 1.000 | 1.353 | 0.000 | 2.557 | 5.370 | 0.07305 | ****** | 56.075 | 6482984 | 0.5157 | ****** | ****** | ****** | 5.568 | 23.271 | 0.031 |
| 1.050 | 1.357 | 0.000 | 2.631 | 5.408 | 0.07369 | ****** | 54.225 | 6346052 | 0.4918 | ****** | ****** | ****** | 5.568 | 23.268 | 0.028 |
| 1.100 | 1.368 | 0.000 | 2.781 | 5.482 | 0.07492 | ****** | 50.249 | 6054113 | 0.4434 | ****** | ****** | ****** | 5.567 | 23.261 | 0.021 |
| 1.150 | 1.390 | 0.000 | 3.013 | 5.591 | 0.07669 | ****** | 43.597 | 5566497 | 0.3699 | ****** | ****** | ****** | 5.566 | 23.254 | 0.014 |
| 1.200 | 1.425 | 0.000 | 3.247 | 5.694 | 0.07837 | ****** | 35.984 | 4995845 | 0.2943 | ****** | ****** | ****** | 5.565 | 23.250 | 0.010 |
| 1.075 | 1.361 | 0.000 | 2.695 | 5.440 | 0.07422 | ****** | 52.569 | 6223987 | 0.4711 | ****** | ****** | ****** | 5.568 | 23.266 | 0.026 |
| 1.100 | 1.368 | 0.000 | 2.782 | 5.483 | 0.07493 | ****** | 50.243 | 6053277 | 0.4433 | ****** | ****** | ****** | 5.567 | 23.263 | 0.023 |
| 1.125 | 1.377 | 0.000 | 2.892 | 5.535 | 0.07579 | ****** | 47.204 | 5830660 | 0.4086 | ****** | ****** | ****** | 5.567 | 23.259 | 0.019 |
| 1.150 | 1.390 | 0.000 | 3.016 | 5.592 | 0.07673 | ****** | 43.578 | 5564347 | 0.3695 | ****** | ****** | ****** | 5.566 | 23.255 | 0.015 |
| 1.175 | 1.407 | 0.000 | 3.139 | 5.647 | 0.07762 | ****** | 39.691 | 5275939 | 0.3300 | ****** | ****** | ****** | 5.565 | 23.251 | 0.011 |
| 1.200 | 1.425 | 0.000 | 3.247 | 5.694 | 0.07838 | ****** | 35.980 | 4995644 | 0.2942 | ****** | ****** | ****** | 5.565 | 23.247 | 0.007 |
| 1.225 | 1.443 | 0.000 | 3.332 | 5.730 | 0.07895 | ****** | 32.817 | 4751107 | 0.2650 | ****** | ****** | ****** | 5.564 | 23.244 | 0.004 |
| 1.250 | 1.460 | 0.000 | 3.392 | 5.755 | 0.07935 | ****** | 30.376 | 4557674 | 0.2431 | ****** | ****** | ****** | 5.564 | 23.242 | 0.002 |
| 1.275 | 1.473 | 0.000 | 3.432 | 5.772 | 0.07961 | ****** | 28.634 | 4416558 | 0.2279 | ****** | ****** | ****** | 5.563 | 23.240 | 0.000 |
| 1.300 | 1.482 | 0.000 | 3.458 | 5.783 | 0.07978 | ****** | 27.460 | 4319743 | 0.2177 | ****** | ****** | ****** | 5.563 | 23.239 | -0.001 |
| 1.325 | 1.489 | 0.000 | 3.474 | 5.789 | 0.07989 | ****** | 26.698 | 4256153 | 0.2112 | ****** | ****** | ****** | 5.563 | 23.239 | -0.001 |
| 1.350 | 1.493 | 0.000 | 3.484 | 5.793 | 0.07995 | ****** | 26.216 | 4215593 | 0.2071 | ****** | ****** | ****** | 5.563 | 23.238 | -0.002 |
| 1.375 | 1.496 | 0.000 | 3.490 | 5.796 | 0.07999 | ****** | 25.917 | 4190209 | 0.2046 | ****** | ****** | ****** | 5.563 | 23.238 | -0.002 |
| 1.400 | 1.497 | 0.000 | 3.494 | 5.797 | 0.08002 | ****** | 25.732 | 4174513 | 0.2030 | ****** | ****** | ****** | 5.563 | 23.238 | -0.002 |
| 1.425 | 1.498 | 0.000 | 3.496 | 5.798 | 0.08003 | ****** | 25.619 | 4164880 | 0.2020 | ****** | ****** | ****** | 5.563 | 23.238 | -0.002 |
| 1.450 | 1.499 | 0.000 | 3.498 | 5.799 | 0.08004 | ****** | 25.550 | 4158994 | 0.2015 | ****** | ****** | ****** | 5.563 | 23.238 | -0.002 |
| 1.500 | 1.500 | 0.000 | 3.499 | 5.800 | 0.08005 | ****** | 25.482 | 4153230 | 0.2009 | ****** | ****** | ****** | 5.563 | 23.238 | -0.002 |
| 1.550 | 1.500 | 0.000 | 3.500 | 5.800 | 0.08005 | ****** | 25.457 | 4151091 | 0.2007 | ****** | ****** | ****** | 5.563 | 23.238 | -0.002 |
| 1.600 | 1.500 | 0.000 | 3.500 | 5.800 | 0.08005 | ****** | 25.448 | 4150302 | 0.2006 | ****** | ****** | ****** | 5.563 | 23.238 | -0.002 |
| 1.650 | 1.500 | 0.000 | 3.500 | 5.800 | 0.08005 | ****** | 25.445 | 4150013 | 0.2006 | ****** | ****** | ****** | 5.563 | 23.238 | -0.002 |

Figure 6. Calculation of pressure and temperature variations in an insulated channel of variable diameter (approximate shape of a venturi).

## 3.5 The Ledinegg Instability

A number of possible instabilities in helium flow systems were outlined and discussed by Steward (unpublished report). Of these, the Ledinegg instability has been studied directly through the use of our program.

The Ledinegg instability refers to a situation which can occur when the fluid enters the heated passage as a dense liquid, with density almost independent of enthalpy, and picks up enough heat while flowing through the channel to emerge from the downstream end in a gas-like state, with a density approximately inversely proportional to enthalpy. For a given mass flow, the gas-like fluid will be moving at relatively high velocity, giving rise to a locally high pressure gradient due to fluid friction. As a result, it is possible that the total pressure drop across the pipe, i.e., the integral of the pressure gradient along its length, could increase if the mass flow is decreased such that a longer fraction of the pipe length contains fluid in the gas-like state [Ledinegg, 1954, and Zuber, 1966]. In effect, such a heated pipe would have a negative resistance characteristic over at least a portion of its flow range. It is well known that a component with negative resistance characteristic will promote unstable system operation.

Most prior studies have been concerned with two-phase fluid flow, wherein a significant quantity of vapor has been formed from boiling liquid within the tube. For a supercritical fluid, the analogous situation is for the thermodynamic state of the fluid to cross the transposed critical line between entrance and exit from the heated flow channel. Prior analyses for this latter case have used crude approximations to the equation of state for the fluid, resulting in the qualitative prediction that Ledinegg instability may likewise occur with a supercritical fluid. Zuber

further shows graphs from experimental work of Krasiakova and Glusker [1965] and Semenkover [1964] with supercritical water supporting this contention, though experimental scatter in the data leaves some room for question.

Our computer program allows a significant advance in the analysis of the supercritical Ledinegg instability, specifically because it uses the exact equation of state of the fluid. We have applied it to the particular case of the superconducting power line, using funding from Brookhaven National Laboratory, and subsequently have been continuing the study in a more general sense under the ARPA funding. One would expect that the occurrence of the instability would become more likely as the integration path on the P - T plane crosses the transposed critical line closer to the critical point, since the transition from liquid-like to gas-like behavior becomes more sharp under these conditions. Surprisingly to us, we have not yet been able to find any conditions of flow, heat flux, input pressure and temperature, channel diameter, etc., which leads to a negative resistance characteristic.

Our analysis will be completed within the next three months and published separately. At this time we can say that the Ledinegg instability should not occur for supercritical helium as easily as previously supposed, and tentatively we feel that it would not be seen outside of the two-phase flow regime.

### 3.6 High Velocity Flow

While testing our computer-generated solutions to the flow equations, we were surprised at the number of times which seemingly reasonable input conditions led to sonic velocity not too far down a pipe of constant diameter. An illustrative output from one such computer run is shown in figure 7; actually it is a fine-grained integration of the tail

HELIUM FLOW AND HEAT TRANSFER
PIPE DIAMETER = 0.5000 CM
FLOW RATE = 0.5000 G/S OR 2.5465 G/CM2S
MINIMUM INTEGRATION ACCURACY =0.00300
WALL HEAT FLUX = 0.15708 W/M

| | Z METERS | P ATMOS | T K | Q WATT | V M/S | HSTAG J/GM | DELT K | DS(DELT) J/GM K | DS(FRACT) J/GM K | S J/GM K | HERROR J/GM |
|---|---|---|---|---|---|---|---|---|---|---|---|
| | 0.000 | 0.255 | 51.951 | 0.000 | 106.417 | 290.141 | 0.017 | 0.000 | 0.000 | 25.142 | 0.000 |
| | 0.200 | 0.238 | 51.814 | 0.031 | 113.497 | 290.203 | 0.017 | 0.000 | 0.124 | 25.268 | -0.000 |
| * | 0.400 | 0.220 | 51.625 | 0.063 | 122.339 | 290.266 | 0.017 | 0.000 | 0.268 | 25.413 | -0.000 |
| * | 0.600 | 0.200 | 51.353 | 0.094 | 133.879 | 290.329 | 0.017 | 0.000 | 0.438 | 25.584 | -0.000 |
| * | 0.800 | 0.177 | 50.923 | 0.126 | 150.003 | 290.382 | 0.017 | 0.000 | 0.647 | 25.794 | -0.010 |
| | 0.300 | 0.230 | 51.727 | 0.047 | 117.653 | 290.235 | 0.017 | 0.000 | 0.193 | 25.338 | -0.000 |
| | 0.400 | 0.220 | 51.625 | 0.063 | 122.339 | 290.266 | 0.017 | 0.000 | 0.268 | 25.413 | -0.000 |
| | 0.500 | 0.211 | 51.503 | 0.079 | 127.687 | 290.298 | 0.017 | 0.000 | 0.349 | 25.494 | -0.000 |
| | 0.600 | 0.200 | 51.353 | 0.094 | 133.079 | 290.329 | 0.017 | 0.000 | 0.438 | 25.584 | -0.000 |
| | 0.700 | 0.189 | 51.166 | 0.110 | 141.180 | 290.360 | 0.017 | 0.000 | 0.536 | 25.683 | -0.001 |
| | 0.800 | 0.177 | 50.925 | 0.126 | 149.998 | 290.391 | 0.017 | 0.000 | 0.647 | 25.794 | -0.001 |
| * | 0.900 | 0.164 | 50.601 | 0.141 | 161.001 | 290.420 | 0.017 | 0.000 | 0.773 | 25.921 | -0.003 |
| * | 1.000 | 0.149 | 50.140 | 0.157 | 175.406 | 290.447 | 0.017 | 0.000 | 0.922 | 26.071 | -0.000 |
| * | 1.100 | 0.132 | 49.414 | 0.173 | 195.808 | 290.468 | 0.017 | 0.000 | 1.105 | 26.254 | -0.026 |
| | 0.850 | 0.171 | 50.776 | 0.134 | 155.168 | 290.406 | 0.017 | 0.000 | 0.708 | 25.855 | -0.001 |
| | 0.900 | 0.164 | 50.682 | 0.141 | 161.000 | 290.422 | 0.017 | 0.000 | 0.773 | 25.921 | -0.001 |
| | 0.950 | 0.157 | 50.394 | 0.149 | 167.663 | 290.438 | 0.017 | 0.000 | 0.844 | 25.993 | -0.001 |
| | 1.000 | 0.149 | 50.142 | 0.157 | 175.402 | 290.453 | 0.017 | 0.000 | 0.922 | 26.071 | -0.002 |
| | 1.050 | 0.141 | 49.826 | 0.165 | 184.581 | 290.468 | 0.017 | 0.000 | 1.008 | 26.157 | -0.002 |
| * | 1.100 | 0.132 | 49.419 | 0.173 | 195.791 | 290.482 | 0.017 | 0.000 | 1.105 | 26.254 | -0.004 |
| * | 1.150 | 0.121 | 48.863 | 0.181 | 210.075 | 290.494 | 0.017 | 0.000 | 1.216 | 26.365 | -0.008 |
| * | 1.200 | 0.109 | 48.037 | 0.188 | 229.595 | 290.496 | 0.017 | 0.000 | 1.347 | 26.497 | -0.022 |
| | 1.075 | 0.137 | 49.637 | 0.169 | 189.882 | 290.476 | 0.017 | 0.000 | 1.055 | 26.204 | -0.002 |
| | 1.100 | 0.132 | 49.419 | 0.173 | 195.790 | 290.484 | 0.017 | 0.000 | 1.105 | 26.254 | -0.002 |
| | 1.125 | 0.127 | 49.165 | 0.177 | 202.451 | 290.492 | 0.017 | 0.000 | 1.158 | 26.308 | -0.002 |
| | 1.150 | 0.121 | 48.864 | 0.181 | 210.071 | 290.499 | 0.017 | 0.000 | 1.216 | 26.365 | -0.003 |
| | 1.175 | 0.116 | 48.499 | 0.185 | 218.953 | 290.507 | 0.017 | 0.000 | 1.278 | 26.428 | -0.003 |
| * | 1.200 | 0.109 | 48.042 | 0.188 | 229.578 | 290.513 | 0.017 | 0.000 | 1.347 | 26.497 | -0.004 |
| * | 1.225 | 0.102 | 47.442 | 0.192 | 242.785 | 290.518 | 0.017 | 0.000 | 1.424 | 26.574 | -0.007 |
| * | 1.250 | 0.093 | 46.595 | 0.196 | 260.268 | 290.517 | 0.017 | 0.000 | 1.512 | 26.662 | -0.017 |
| | 1.188 | 0.113 | 48.284 | 0.187 | 224.007 | 290.511 | 0.017 | 0.000 | 1.312 | 26.462 | -0.003 |
| | 1.200 | 0.109 | 48.042 | 0.188 | 229.577 | 290.515 | 0.017 | 0.000 | 1.347 | 26.497 | -0.003 |
| | 1.213 | 0.106 | 47.765 | 0.198 | 235.781 | 290.519 | 0.017 | 0.000 | 1.384 | 26.534 | -0.003 |
| | 1.225 | 0.102 | 47.443 | 0.192 | 242.781 | 290.522 | 0.017 | 0.000 | 1.424 | 26.574 | -0.003 |
| | 1.238 | 0.098 | 47.062 | 0.194 | 250.814 | 290.526 | 0.017 | 0.000 | 1.466 | 26.617 | -0.004 |
| * | 1.250 | 0.093 | 46.598 | 0.196 | 260.253 | 290.529 | 0.017 | 0.000 | 1.512 | 26.662 | -0.004 |
| * | 1.263 | 0.088 | 46.011 | 0.198 | 271.737 | 290.531 | 0.017 | 0.000 | 1.562 | 26.713 | -0.006 |
| * | 1.275 | 0.082 | 45.214 | 0.200 | 286.547 | 290.529 | 0.017 | 0.000 | 1.618 | 26.769 | -0.012 |
| | 1.244 | 0.096 | 46.843 | 0.195 | 255.326 | 290.528 | 0.017 | 0.000 | 1.489 | 26.639 | -0.004 |
| | 1.250 | 0.093 | 46.598 | 0.196 | 260.252 | 290.530 | 0.017 | 0.000 | 1.512 | 26.662 | -0.004 |
| | 1.256 | 0.091 | 46.324 | 0.197 | 265.680 | 290.532 | 0.017 | 0.000 | 1.537 | 26.687 | -0.004 |
| | 1.263 | 0.088 | 46.011 | 0.198 | 271.734 | 290.534 | 0.017 | 0.000 | 1.562 | 26.713 | -0.004 |
| | 1.269 | 0.086 | 45.648 | 0.199 | 278.592 | 290.535 | 0.017 | 0.000 | 1.590 | 26.740 | -0.004 |
| * | 1.275 | 0.082 | 45.217 | 0.200 | 286.533 | 290.537 | 0.017 | 0.000 | 1.618 | 26.769 | -0.004 |
| * | 1.281 | 0.079 | 44.684 | 0.201 | 296.034 | 290.537 | 0.017 | 0.000 | 1.649 | 26.799 | -0.006 |
| * | 1.288 | 0.075 | 43.985 | 0.202 | 308.040 | 290.536 | 0.017 | 0.000 | 1.683 | 26.833 | -0.009 |
| | 1.272 | 0.084 | 45.443 | 0.200 | 282.403 | 290.536 | 0.017 | 0.000 | 1.604 | 26.754 | -0.004 |
| | 1.275 | 0.082 | 45.217 | 0.200 | 286.532 | 290.537 | 0.017 | 0.000 | 1.618 | 26.769 | -0.004 |
| | 1.278 | 0.081 | 44.966 | 0.201 | 291.044 | 290.538 | 0.017 | 0.000 | 1.633 | 26.784 | -0.004 |
| | 1.281 | 0.079 | 44.684 | 0.201 | 296.030 | 290.539 | 0.017 | 0.000 | 1.649 | 26.799 | -0.004 |
| | 1.284 | 0.077 | 44.363 | 0.202 | 301.623 | 290.540 | 0.017 | 0.000 | 1.665 | 26.816 | -0.004 |
| | 1.288 | 0.075 | 43.987 | 0.202 | 308.028 | 290.541 | 0.017 | 0.000 | 1.683 | 26.833 | -0.005 |
| | 1.291 | 0.072 | 43.533 | 0.203 | 315.595 | 290.541 | 0.017 | 0.000 | 1.701 | 26.851 | -0.005 |
| | 1.294 | 0.069 | 42.951 | 0.203 | 325.026 | 290.540 | 0.017 | 0.000 | 1.723 | 26.870 | -0.007 |
| | 1.297 | 0.065 | 42.108 | 0.204 | 338.211 | 290.533 | 0.018 | 0.000 | 1.741 | 26.891 | -0.015 |

FLUID REACHES SONIC VELOCITY

ASTERISKS INDICATE CALCULATED POINTS WHICH ARE SUBSEQUENTLY CORRECTED

Figure 7. Calculation of pressure and temperature profiles as the helium flow approaches sonic velocity.

end of a previous run using a much more coarse grid. It is seen that the velocity increases very rapidly with small increments in the axial coordinate as the position of the shock front is approached.

A basic assumption in the derivation of the equation is that the fluid is in local thermodynamic equilibrium within each differential fluid element of length dz and diameter D. This assumption is may be invalid very near the shock front where the predicted fluid properties change significantly in a length comparable to the channel diameter. Nevertheless the equations maintain mathematical consistency right up to Mach 1.

To investigate the effects of friction and heat transfer on the development of a shock, consider just a straight pipe for which case eq (12) can be written

$$\frac{\partial M}{\partial z} = \frac{\frac{p}{2a}\left(1 - \frac{c^2}{\omega^2}\right) f M^3 + \frac{qp}{a\rho\omega^2 c}}{1 - M^2} . \qquad (15)$$

It is further convenient to use a reduced coordinate $z^* = z/(4a/p)$, where the denominator is the hydraulic diameter of the flow passage. Separating variables, the equation becomes:

$$dz^* = \frac{1}{2\left(1 - \frac{c^2}{\omega^2}\right)} \frac{1 - M^2}{(fM^3 + QM)} dM$$

where

$$Q = \frac{2q}{G\omega c\left(1 + \frac{c^2}{\omega^2}\right)} .$$

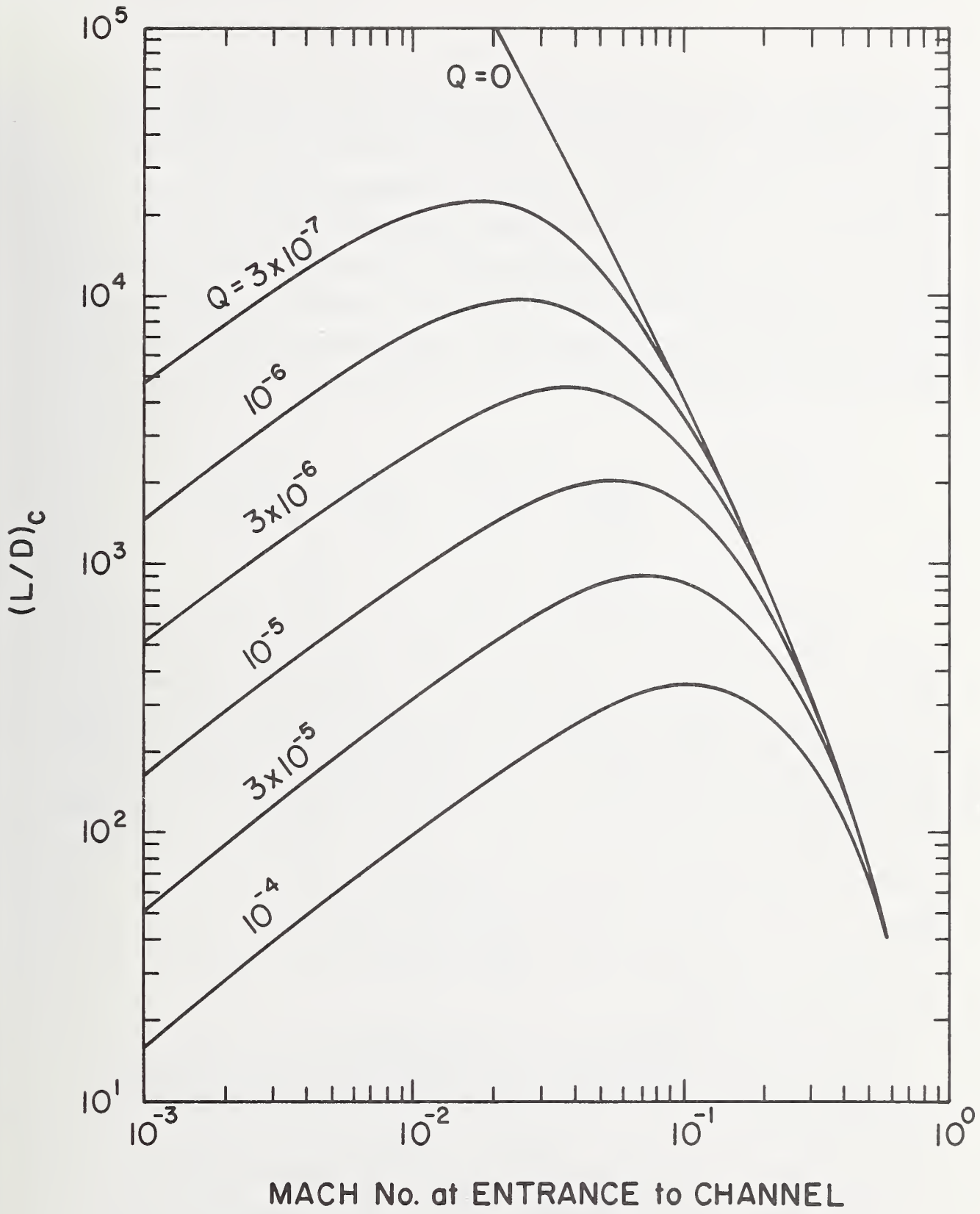


Figure 8. Critical channel lengths within which the helium reaches sonic velocity, as a function of helium velocity at the input. Q is a dimensionless heating rate defined in the text.

Conveniently, for a reasonable range of pressures, temperatures, and flows in helium-cooled systems, the velocities $\omega$ and c and the friction factor are roughly constant (f has never really been measured as $M \rightarrow 1$, but the trend at lower flows is to become constant as the flow increases). Thus, for an approximate estimate of the channel length over which sonic velocity is reached, Q and f can be treated as constants, and the integration is straightforward, though tedious. Assuming $M = M_o$ at $z^* = 0$ and $M = 1$ at $z^* = (L/D)_c$, the result is

$$2\left(1 + \frac{c^2}{\omega^2}\right)\left(\frac{L}{D}\right)_c = \frac{1}{2f} \ln\left(\frac{Q + M_o^2 f}{Q + f}\right) + \frac{1}{2Q} \ln\left(\frac{Q + M_o^2 f}{M_o^2 (Q + f)}\right)$$

The dimensionless factor Q can vary over a wide range with different cooling systems and designs. A reasonable range would be perhaps $10^{-4}$ as a maximum down to about $10^{-7}$. With no heat transfer, $Q = 0$. Figure 8 shows $(L/D)_c$ for a wide range of values of Q, assuming $f = 0.003$. At very low flow, for a given heat input, the fluid warms to low density and sonic velocity in a relatively short length. At a very high flow, fluid friction alone lends to sonic velocity. Obviously no system would be designed close to the limit suggested by these approximate curves, but this limit could become very important when it comes to off-design, overload conditions in long channels, e.g., superconducting power lines.

### 3.7 The Polytropic Approximation

Some problems on fluid flow have been studied in the polytropic approximation,

$$\frac{\rho}{P} \frac{dP}{d\rho} = n$$

where the index n is correlated with the type of process involved, i. e. ,

n = 0 for an isobaric process

n = 1 for an isothermal process

n = $\gamma$ for an isentropic process

n = $\infty$ for an isovolumetric process.

It is useful to evaluate the polytropic index n for the general case of fluid flowing through a heated (or cooled) conduit. Simple substitution from the eqs (8) and (11), and using thermodynamic definitions, yields the exact result

$$n = \frac{\gamma}{Pk} \frac{f_e\left(1+\frac{U^2}{\omega^2}\right) + \frac{2q_e}{\rho\omega^2 U}}{f_e\left(1+\frac{c^2}{\omega^2}\right) + \frac{2q_e c^2}{\rho\omega^2 U^3}} . \qquad (16)$$

We can now evaluate this for several approximations.

When there is no heat transfer between the fluid and the conduit, and the cross section is constant, $q_e = 0$, and the polytropic index becomes

$$n = \frac{1+\frac{U^2}{\omega^2}}{1+\frac{c^2}{\omega^2}} \cdot \frac{\gamma}{Pk} \qquad (17)$$

For an ideal gas, this reduces to n = 1 in the limit of small velocities, and n = $\gamma$ in the limit U $\rightarrow$ c. Both of these are in accord with known results [Chivers and Mitchell, 1971].

For flow in which heat is added (or taken from) the moving fluid, and/or for flow through a conduit of changing cross section, three

regimes can be identified depending on the relative magnitude of the terms in eq (16). When the flow velocity is much less than a lower crit cal velocity, $M_1$, given approximately by

$$M_1 = \frac{U_1}{c} \approx \frac{2q_e}{\rho f_e \omega^2 c} \tag{18}$$

we obtain the result,

$$n \approx \frac{\gamma}{Pk} \cdot M^2 \tag{19}$$

When the flow velocity is much greater than an upper velocity, $M_2$, given approximately by

$$M_2 \approx \left( \frac{M_1}{1 + \frac{c^2}{\omega^2}} \right)^{1/3} . \tag{20}$$

we obtain eq (17), which applies when the heat transfer is negligible with respect to kinetic effects.

When the flow velocity is between the two values $M_1$ and $M_2$, the index is approximately

$$n \approx \frac{\gamma}{Pk} \frac{f_e \left(1 + \frac{U^2}{\omega^2}\right)}{2} \frac{G \omega^2 M^2}{q_e} . \tag{21}$$

The following table gives approximate values of $U_1$ and $U_2$ for turbulent helium flow in the range 4 - 10 K, 1 - 5 atmospheres, using the approximation $c \approx \omega \approx 150$ m/s.

| $q[W/cm^2]$ | $U_2$ [m/s] | $U_1$ [m/s] |
|---|---|---|
| 3. | 50 | 5 |
| 1. | 35 | 1.5 |
| 0.1 | 15 | 0.5 |
| 0.01 | 8 | 0.05 |

Heat fluxes encountered in design are typically under 1 $W/cm^2$, while flow velocities required for reasonable heat transfer rates will be $\geq$ 1 m/s. This suggests that typical designs will have $U_1 \leq U < U_2$. It is worthwhile to consider the polytropic equation in more detail for this case.

Using the approximation $U^2/\omega^2 \ll 1$, and considering just a straight tube for which $\rho U = G$ = constant, we find

$$k dP \approx -\gamma d\left(\tfrac{1}{2} M^2\right)\left(1 + \frac{f\omega^2 G}{2q}\right). \qquad (22)$$

This is a useful relationship between the pressure drop and the change in kinetic energy for general, non-ideal flow in a conduit.

### 3.8 Time Dependent Problems

We have given serious attention to integration of the time-dependent equations 2, 3, and 6, for studies of transient effects in the cooling of superconducting systems (flux jumps, for example). One such problem which particularly needs study is the growth or decay

of a finite-length normal region of superconductor cooled by forced flow [Arp, 1972]. Two previous studies on this topic have both used a mathematical approach which rules a direct recovery process which we think would be operative with forced single-phase flow [Greene and Saibel, 1968, and Bald, 1970].

Basically, the mathematical procedure involves integration over the spatial coordinate, sometimes iterating to match boundary conditions, once at each increment of time. This problem can be very time consuming because we want to avoid approximations to the fluid equation of state.

After working with this problem for a while, we have concluded that the integration could be performed more rapidly, at least when the kinetic energy terms can be neglected, if enthalpy rather than temperature were one of the independent parameters of the equation of state. This comes about because the enthalpy change is equal to the heat input from the superconductor, and one iteration step could be eliminated. Though this is not a critical factor in doing this particular calculation, we came to realize from this work that iterative steps in a great body of helium flow and refrigeration calculations can be eliminated by having available different forms for the equation of state. Accordingly, we have decided that the ARPA program would best be advanced by setting aside, temporarily, this particular time-dependent flow calculation and concentrating instead on the development of appropriate new forms of the equations of state. This work is described in the following section.

## 4.0 Helium State Equations For Refrigeration Analysis

The basic equations of state for the properties of helium has been given by McCarty [1972, 1973]. This work will undoubtedly stand for

some time as the fundamentally accurate helium state equation, giving both the PVT surface and properties such as specific heats, compressibilities, etc., which are related to the derivatives of the PVT surface. The refrigeration cycles analyses and helium flow analyses discussed in this report have all been performed using McCarty's equations.

For practical analysis of refrigeration and flow problems, however, the independent state parameters should be the enthalpy (related to heat input), pressure (related to flow friction factors) and sometimes the entropy (related to system reversibility), rather than the density and the temperature which are the independent parameters of McCarty's equations. This is in no sense a criticism of McCarty's work since all fundamental theories and equations of fluid properties are based on density and temperature expansions. But as a result, the equations are very cumbersome to use in engineering analysis. For example, a double iteration must be done to find density and temperature and then other properties of interest from a given pressure and enthalpy. Such procedure is time consuming and very costly, and has been a significant limitation to the refrigeration and fluid flow analysis to date.

As a result, we have spent some time developing three new state equations for helium based on McCarty's work. We call these (1) S (P,H) which calculates entropy from pressure and enthalpy, (2) H (P,S), which calculates enthalpy from pressure and entropy, and (3) T(P,H), which calculates temperature from pressure and enthalpy. In the future we plan to add one more, V (P,H), which will calculate the specific volume.

In order to develop these, within just the last 3 to 4 months, we have adopted guidelines which differ from McCarty's in several respects:

(1) The equations should be reliable for engineering calculations, but need not retain the fundamental accuracy of McCarty's equations.

(2) Each relationship should be expressed by a single mathematical equation over the entire range of interest. McCarty, on the other hand, uses three separate equations covering three different regions of the pressure-temperature plane, with careful splicing techniques to obtain smooth transitions from one equation to the next in the regions of overlap. This system of equations is not easily programmed for the computer.

(3) McCarty's equations are structured so that it is reasonably easy to take derivatives of the PVT surface. We have not retained this requirement, thus making it much easier to find products of mathematical functions yielding reasonable fit of the stated variables, but whose derivatives contain many factors and are algebraically complex.

(4) McCarty's equations cover the ranges 2 to 1500 K and 0 to 1000 atmospheres. For studies of helium refrigeration cycles, there is little impetus to go to pressures above about 50 atmospheres. Our fitting is done to 100 atmospheres, but weighted by the factor $2./\ (1.0 + P^{0.25})$, emphasizing the lower pressures. Our temperature range is from 3 to 400 K, though in fact they retain reasonable accuracy considerably above 400 K.

The analysis was performed with a linear general least-squares fitting program which determines the best coefficients for up to 36 independently-specified functions. Consistent with the above guidelines, we have found it necessary in some cases to include additional numerical constants within the specified functions in order to obtain desirable accuracy in the result. These nonlinear constants were selected by intermediate-stage studies, often of intuitive nature, with some repeated testing to obtain approximate numerical values which optimize the fit. Accurate optimization of these nonlinear constants would be intolerably expensive and probably would not gain much.

At this stage, we have not completed all the statistical analyses and tests of the results, etc., nor have we obtained even an approximate equation V(P,H). This will be completed within the next few months and submitted for separate publication. The equations are presented here for those who may wish to use them in engineering calculations without waiting for full documentation.

Throughout all the numerical equations, pressures are in atmospheres, enthalpies in J/g, and entropies in J/gK.

### 4.1 Structure of the Equations

At temperatures above 300 K, helium behaves very nearly as an ideal gas, and some rather simple expressions are found to satisfy the equations at all pressures up to 100 atmospheres. We give these here for further reference.

For an ideal gas, the enthalpy is just equal to the integral of specific heat with respect to temperature, independent of pressure, with one constant of integration. From McCarty's equations, we find, for pressures up to 100 atmospheres, at T = 300 K,[1]

$$T = \frac{H}{C_{pi}} - 2.82446 - 0.064533\,P + 5.800 \times 10^{-6} P^2,$$

and at T = 350 K,

$$T = \frac{H}{C_{pi}} - 2.82419 - 0.064617\,P + 5.686 \times 10^{-6} P^2,$$

and at T = 400 K,

$$T = \frac{H}{C_{pi}} - 2.82394 - 0.064469\,P + 5.615 \times 10^{-6} P^2 \qquad (23)$$

where $C_{pi} = (5/2)R = (5/2) \times 2.0772258$ J/g·K. (24)

---

[1] Throughout these calculations we retain more significant figures than justified by the basic experimental data, in order to avoid roundoff error in the calculated expressions.

The differences between these equations are unimportant for this work, indicating that one set of these parameters can reasonably fit the helium data in the room temperature range. We have arbitrarily used the last equation, evaluated at 400 K, in subsequent work. The standard deviation between this expression and the 400 K data is 0.000181 K.

The entropy of an ideal gas is given by

$$S_i = S_o + C_p \ln\left(\frac{T}{T_o}\right) - R \ln\left(\frac{P}{P_o}\right)$$

We find that McCarty's equations can be fitted at both 300 K and 400 K up to 100 atmospheres by

$$S_i = C_{pi} \ln T - R \ln P + 1.79056 + 0.0001077\, P \qquad (25)$$

to an accuracy of about 0.002%. Using eq (23) to eliminate T, the "ideal" relationship between H and S is found to be

$$H_i = 3.6785757\, P^{0.4} \exp\left(\frac{S_i - 0.0001077 P}{C_{pi}}\right) + 14.6649 + 0.33479\, P - 0.00002913\, P^2 \qquad (26)$$

This expression can readily be inverted to give $S_i(H_i, P)$.

One additional subsidiary equation turns out to be necessary for this work.

Figure 4 shows the specific heat of helium as function of temperature for several pressures in the neighborhood of the critical point (5.2014 K, 2.245 atmospheres). The loci of the peaks of the

specific heat curves, as a function of pressure and temperature, define the transposed critical line, in the neighborhood of which all real properties show unusually strong dependencies on pressure and temperature in a narrow range. In order to obtain equations free of significant error in the vicinity of the transposed critical line, it is necessary to add knowledge of its existence into the equations in some form. In this work it is done by evaluating the enthalpy at the transposed critical line as a function of pressure. Calling this quantity $H_{tc}$, its equation is

$$H_{tc} = 16.3713 + 2.21774\ P - 0.002606\ P^2 \qquad (27)$$

with a weighted standard deviation of about 0.8 joules per gram. This equation is probably much more precise than the accuracy with which $H_{tc}$ is really known from experimental work. However, it is also slightly uncertain due to a slight lack of thermodynamic consistency which we have found in McCarty's equations at higher pressures, as explained in more detail in the discussion of equation T (P,H). In the equations to follow, it is convenient to use a reduced enthalpy, h, given by

$$h = H / H_{tc} . \qquad (28)$$

The subsequent equations for the properties of the real fluid are developed from the differences between the real fluid property and that given by the appropriate pressure-dependent "ideal gas" equation above. In developing these equations, one cannot avoid exploring a number of mathematical approaches which turn out to be unprofitable. We give here only our best results to date (June 15, 1973).

## 4.2 Function T (P, H)

Figure 9 shows the difference between the temperature and that predicted by the "ideal gas" eq (23), for several different pressures. It looks somewhat like a Gaussian function, $\exp(-a \cdot x^2)$ or Lorentzian function $(1-a \cdot x^2)^{-1}$, whose center position $H_{cpi}$ is a function of pressure. Conveniently, its shape is not qualitatively changed as it bridges the two-phase region.

While exploring these features, we uncovered a small error in McCarty's work which needs some explanation. The center position of the above Gaussian or Lorenzian curves can be obtained in two ways. One way is to read the $H(y_{max})$ directly from large and carefully plotted graphs equivalent to figure 9. Secondly, one can use the fact that at the center position the specific heat of the real fluid must equal that of the ideal gas, as can be shown using just the thermodynamic definition $C_p = (\partial H/\partial T)_p$ and simple differentiation. However, we found that the center positions determined by the two methods differed by as much as 10% in enthalpy in the range of pressures of roughly 30 to 60 atmospheres.

After further study and discussion with McCarty, we deduce that this thermodynamic inconsistency occurs only in the temperature range from 10 to 15 K where two of his primary equations overlap and were thought to be smoothly joined. Apparently there is a residual error in the joining which shows up in this rather sensitive test.

The final data to which our equation for $H_{cpi}$ is fitted were selected by excluding the region from 10 to 15 K, which in effect excludes the region from about 30 to 60 atmospheres. The fitting was done to points at 5, 10, 15, 20, 25, 70, 80, 90, and 100 atmospheres. At all of these points except the first one the agreement between the two methods for determining $H(Y_{max})$ was about equal to the accuracy of the graphical

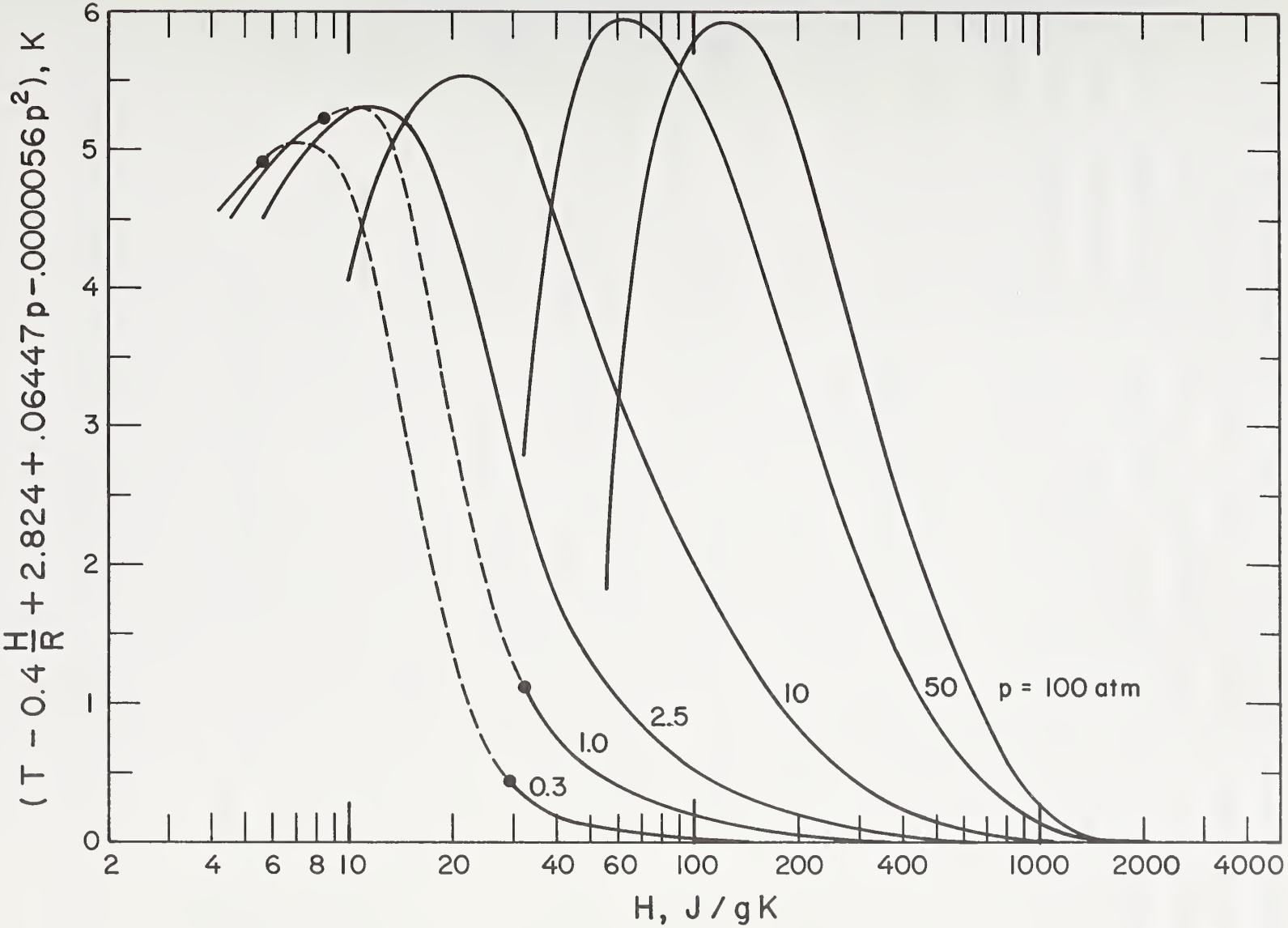


Figure 9. Difference between the true temperature and the "ideal gas temperature" at the same enthalpy and pressure, as defined in the text.

method used, or about 1% or better. At 5 atmospheres there was a small but distinct difference between the two, the zero-slope method giving 14.3 J/g and the Cp method giving 14.95 J/g, with the best smooth curve predicting 15.2 J/g. We speculate that these differences are due to small residual inaccuracies in McCarty's equations as the critical point is approached; such inaccuracies are undoubtedly minor in comparison with uncertainties in the experimental data to which the equations are fitted.

At 30 to 50 atmospheres, the fitted curve turns out to agree to within about 0.6 J/g with the values deduced from $C_p$ values at these pressures, but differs by 3.3 and 6.7 J/g respectively from that determined by the zero-slope method. The equation is

$$H_{cpi} = 8.6467 + 1.3220\,P - 0.001823\,P^2 \qquad (29)$$

with an rms error of 0.34 J/g between fitted and calculated points. In the fitted equation we use a reduced enthalpy in some terms.

$$\phi = (H / H_{cpi}) \qquad (30)$$

Various equations and modifications of equations were tested by fitting to 932 data points generated from McCarty's equations. Because of the thermodynamic consistency problems between 10 and 15 K, all points below 20 atmospheres in this range were given weight 0.5, and all those above 20 atmospheres were given weight 0.01 (essentially zero).

The following equation for T (P,H) appears quite complex, since we have in general chosen to expand in a series of terms characterized

by successive values of the nonlinear numerical constants, rather than simpler power series in H and P. We do this because we found we can obtain about three times the accuracy with three less terms using the more complex functions rather than the simpler power series expansions as used in functions S (P,H) and H (P,S). For final use on a computer, the additional complexity is insignificant, whereas the increase in accuracy may be important.

We start by defining functions

$$F_1(x,a) = 1 - \left( \frac{1+(1/w)^a}{1+(x/w)^a} - 1 \right)^2 \quad ; \quad w = 0.6$$

$$F_2(x) = (1 + 0.13711501 \log_e(x/2)) / (1+(x/2)^5)$$

$$F_3(x,a,y,b) = x\, e^{-ax^2}\, e^{-y/b}$$

$$F_4(x) = (\log_e x)^2 / (1+x^3)$$

$$F_5(x) = (\log_e x)^3 / (1+x^3)$$

and a pressure variable

$$p = \log_e(1.0 + P) . \qquad (31)$$

In terms of these functions, the deviations graphed in figure 12 between the true temperature and the ideal temperature $T_i$ given by eq (23) is

$$
\begin{aligned}
(T - T_i) = {} & F_1(\phi, 2.10) \times (a_1 p + a_2 p^2 + a_3 p^3 + a_4 p^4) \\
& + F_1(\phi, 1.85) \times (a_5 p + a_6 p^2 + a_7 p^3) \\
& + F_1(\phi, 1.60) \times (a_8 p + a_9 p^2 + a_{10} p^3) \\
& + F_1(\phi, 1.35) \times (a_{11} p + a_{12} p^2 + a_{13} p^4) \\
& + F_2(\phi) \times (a_{14} e^{-(P/3.)} + a_{15} e^{-(P/3.5)} + a_{16} e^{-(P/4.0)}) \\
& + F_3(\log_e h, 10., P, 4.) \times (a_{17} + a_{18} p + a_{19} p^2 + a_{20} p^3) \\
& + F_3(\log_e h, 4., P, 4.) \times (a_{21} + a_{22} p + a_{23} p^2 + a_{24} p^3) \\
& + F_4(\phi) \times (a_{25} + a_{26} p + a_{27} p^2 + a_{28} p^3 + a_{29} p^4) \\
& + F_5(\phi) \times (a_{30} p + a_{31} p^2 + a_{32} p^3 + a_{33} p^4)
\end{aligned}
\tag{32}
$$

where the constants $a_i$ are given in table 6 . Thus, the true temperature is given by the sum of eq (32) for $(T - T_i)$ and eq (23) for $T_i$, for a given P and H.

The standard deviation between this result and McCarty's defining equations is 0.015 K. The accuracy in the vicinity of the two-phase region is generally 0.006 K or better, and the largest error on the 2.3 atmosphere isobar, near the critical point, is 0.022 K. At higher pressures, the error increases.

Table 6. Numerical constants for the equation T(P,H).

| | | | |
|---|---|---|---|
| $a_1$ = | 13.878902654 | $a_{18}$ = | 6.2461795885 |
| $a_2$ = | -9.1294555014 | $a_{19}$ = | -0.4080674500 |
| $a_3$ = | 1.4753132952 | $a_{20}$ = | -1.1548143734 |
| $a_4$ = | -0.064635371239 | $a_{21}$ = | -2.3614901630 |
| $a_5$ = | -14.085703051 | $a_{22}$ = | 4.6428182119 |
| $a_6$ = | -4.3222209397 | $a_{23}$ = | -2.9101156545 |
| $a_7$ = | 1.4429523076 | $a_{24}$ = | 0.90838981816 |
| $a_8$ = | -1.8712988904 | $a_{25}$ = | -0.23446642474 |
| $a_9$ = | 18.815813408 | $a_{26}$ = | 21.976664669 |
| $a_{10}$ = | -3.3611959286 | $a_{27}$ = | -26.313269947 |
| $a_{11}$ = | 3.2417847568 | $a_{28}$ = | 5.8053275951 |
| $a_{12}$ = | -4.1613166989 | $a_{29}$ = | -0.29763970504 |
| $a_{13}$ = | 0.1053291809 | $a_{30}$ = | 4.5591407995 |
| $a_{14}$ = | 34.867402925 | $a_{31}$ = | -6.5729084580 |
| $a_{15}$ = | -76.900659027 | $a_{32}$ = | 2.0788999721 |
| $a_{16}$ = | 47.935651420 | $a_{33}$ = | -0.17257458796 |
| $a_{17}$ = | -4.6708598724 | | |

## 4.3 The Function H (P,S)

This function takes pressure and entropy as the input variables and calculates enthalpy. The general procedure is to first calculate an "ideal" enthalpy $H_i$ using eq (26). A correction term, $\Delta_1 H$ is calculated from eq (33) shown below, and the final answer is obtained by adding $\Delta_1 H$ to $H_i$. In evaluating the constants for eq (33), the same low weight was given to the points between 10 and 15 K as was described under eq T (P,H).

$$\Delta_1 H = \exp\left(-\frac{S}{C_{Pi}}\right) \sum_{i=1}^{7} \sum_{j=1}^{5} b_{ij} \left(\exp\left(\frac{S}{C_{Pi}}\right)-1\right)^{1-i/3} p^{(j-1)} \qquad (33)$$

where $C_{Pi}$ is the ideal gas specific heat given by eq (24) and p is the pressure variable given by eq (31). The coefficients $b_{ij}$ are given in table 7. Then,

$$H(P,S) = \Delta_1 H + H_i \text{ (eq. 26)} .$$

The standard deviation between the calculated enthalpy and that given by McCarty's program is 0.050 J/g. If we relate this to a temperature error at constant pressure by

$$\delta T = \frac{\delta H}{C_P}$$

the equivalent temperature error is approximately 0.010 K.

Table 7. Numerical constants for the equation H(P,S).

$b_{11} = 6.2095652653 \times 10^{-1}$

$b_{12} = -2.4559275204 \times 10^{1}$

$b_{13} = 2.2297261674 \times 10^{1}$

$b_{14} = -6.7492782747$

$b_{15} = 4.1021573691 \times 10^{-1}$

$b_{21} = -5.2643461931 \times 10^{-2}$

$b_{22} = 3.6216988376 \times 10^{2}$

$b_{23} = -3.2737113461 \times 10^{2}$

$b_{24} = 9.9186574011 \times 10^{1}$

$b_{25} = -7.0819815035$

$b_{31} = -5.2181285811 \times 10^{1}$

$b_{32} = -1.8942905449 \times 10^{3}$

$b_{33} = 1.7107602365 \times 10^{3}$

$b_{34} = -5.0693398133 \times 10^{2}$

$b_{35} = 3.8921676371 \times 10^{1}$

$b_{41} = 2.5428630050 \times 10^{2}$

$b_{42} = 4.5255682326 \times 10^{3}$

$b_{43} = -4.1189023813 \times 10^{3}$

$b_{44} = 1.1828344037 \times 10^{3}$

$b_{45} = -9.3218939174 \times 10^{1}$

$b_{51} = -4.4998406724 \times 10^{2}$

$b_{52} = -5.4945892540 \times 10^{3}$

$b_{53} = 4.9550341804 \times 10^{3}$

$b_{54} = -1.3819212763 \times 10^{3}$

$b_{55} = 1.1001849787 \times 10^{2}$

$b_{61} = 2.9726956809 \times 10^{2}$

$b_{62} = 3.2678083338 \times 10^{3}$

$b_{63} = -2.8933124992 \times 10^{3}$

$b_{64} = 7.8724009925 \times 10^{2}$

$b_{65} = -6.2871925138 \times 10^{1}$

$b_{71} = -6.6277471159 \times 10^{1}$

$b_{72} = -7.5478760174 \times 10^{2}$

$b_{73} = 6.5427817221 \times 10^{2}$

$b_{74} = -1.7447708487 \times 10^{2}$

$b_{75} = 1.3939361536 \times 10^{1}$

## 4.4 The Function S (P,H)

This function takes pressure and enthalpy as the input variables and calculates entropy. The general procedure is to calculate a correction term $\Delta_2 H$ as a function of P, H, and $H_{tc}(P)$, as shown in eq (34) below. This $\Delta_2 H$ is added to the input H to give an "ideal" $H_i$ which in turn is used to calculate S by inverting eq (26). The same low weight was given to points between 10 and 15 K as was described under T (P,H):

$$\Delta_2 H = \sum_{i=1}^{7} \sum_{j=1}^{5} C_{ij} h^{-\left(\frac{3+i}{2}\right)} p^{(j-1)} \qquad (34)$$

where h is the reduced enthalpy given by eq (28) and p is the pressure variable given by eq (31). The coefficients $C_{ij}$ are given in table 8. Then

$$S(P,H) = C_{pi} \log_e \left( \frac{H + \Delta_2 H - 14.6649 - 0.33479\,P + .00002913\,P^2}{3.6785757\,P^{0.4}} \right) + 0.0001077\,P.$$

The standard deviation between the calculated entropy and that given by McCarty's program is 0.017 J/gK. If we relate the error at each data point to a temperature error by

$$\delta T = \left.\frac{\delta T}{\delta S}\right|_P \cdot \delta S = \frac{T}{C_P} \delta S,$$

the standard deviation in temperature is 0.014 K.

Table 8. Numerical constants for the equation S(P,H).

$c_{11}$ = 96.557792404

$c_{12}$ = -85.342124216

$c_{13}$ = 93.239184634

$c_{14}$ = -32.642437375

$c_{15}$ = 2.8950104636

$c_{21}$ = -471.18800861

$c_{22}$ = 337.90821505

$c_{23}$ = -195.19240224

$c_{24}$ = 70.146358374

$c_{25}$ = -6.2193650992

$c_{31}$ = 884.01164347

$c_{32}$ = -359.83067977

$c_{33}$ = -24.961141557

$c_{34}$ = -6.9236428132

$c_{35}$ = 0.4327647102

$c_{41}$ = -821.10597373

$c_{42}$ = 51.518553781

$c_{43}$ = 341.82700671

$c_{44}$ = 90.187334672

$c_{45}$ = 8.3939686508

$c_{51}$ = 405.81584516

$c_{52}$ = 123.84837652

$c_{53}$ = -321.35063183

$c_{54}$ = 89.302684169

$c_{55}$ = -8.2508383745

$c_{61}$ = -102.61607953

$c_{62}$ = -72.105848121

$c_{63}$ = 120.99391576

$c_{64}$ = -34.006661384

$c_{65}$ = 3.140489957

$c_{71}$ = 10.469390204

$c_{72}$ = 11.920614672

$c_{73}$ = -16.687143281

$c_{74}$ = 4.7025518338

$c_{75}$ = -0.4348173542

## 4.5 The Two-Phase Region and Boundaries

The equations presented in sections 4.2 - 4.4 are fitted to helium properties data in both the liquid and the vapor phases, but not in the two-phase region of liquid-vapor equilibrium. When the input data to any one of these equations corresponds to a point in the liquid-vapor equilibrium region, the equations continue to produce numerical results of apparently correct order of magnitude, and an additional test must be made to show that such calculation is in fact meaningless. To do this, we have fitted the following two equations to respectively the enthalpy of the saturated liquid $H_{SL}$ and the enthalpy of the saturated vapor $H_{SV}$ at equilibrium, as a function of pressure. If, for a given pressure, the enthalpy of the fluid is between the two values predicted by these two equations, the point in question is within the two-phase region and the eqs T (P,H), S (P,H), H(P,S), and V(P,H) will give meaningless results. Because eq H (P,S), in particular, is single valued, it can be used as input to these two equations to test whether a given pressure and entropy lies within the two-phase region, even though the calculated enthalpy will be otherwise meaningless within the two-phase region.

$$H_{s\ell} = d_{1\ell}(2.246 - P)^{-1} + \sum_{i=2}^{8} d_{i\ell} P^{(i-2)} \qquad (35)$$

$$H_{sv} = d_{1v}(2.246 - P)^{-1} + \sum_{i=2}^{8} d_{iv} P^{(i-2)} \qquad (36)$$

Table 9. Numerical constants for the equation $H_{SL}(P)$ and $H_{SV}(P)$.

| | |
|---|---|
| $d_{1\ell} = 3.0016449891 \times 10^{-3}$ | $d_{1v} = -1.2529131754 \times 10^{-3}$ |
| $d_{2\ell} = 2.6901274997$ | $d_{2v} = 2.4289246713 \times 10^{1}$ |
| $d_{3\ell} = 1.5023185792 \times 10^{1}$ | $d_{3v} = 2.8759510985 \times 10^{1}$ |
| $d_{4\ell} = -2.4216012980 \times 10^{1}$ | $d_{4v} = -6.6130326207 \times 10^{1}$ |
| $d_{5\ell} = 3.1430206769 \times 10^{1}$ | $d_{5v} = 8.5561182969 \times 10^{1}$ |
| $d_{6\ell} = -2.1707243329 \times 10^{1}$ | $d_{6v} = -6.1554651598 \times 10^{1}$ |
| $d_{7\ell} = 7.4933613037$ | $d_{7v} = 2.2519571060 \times 10^{1}$ |
| $d_{8\ell} = -9.9634989768 \times 10^{-1}$ | $d_{8v} = -3.2937094592$ |

The constants for these equations are given in table 11. The standard deviation is 0.034 J/g at the liquid boundary ($H_{SL}$), and 0.050 J/g at the vapor boundary ($H_{SV}$).

## 4.6 Accuracy

As stated earlier, we have not completed all appropriate tests and measures of the accuracy of these three equations at this time. We can state that the overall inaccuracy, expressed as a temperature error, will generally be less than 0.025 K. More explicit statements can be made about specific regions of the pressure-temperature plane:

(1) The fittings were weighted to provide additional accuracy near the liquid-vapor equilibrium line, where the errors are generally $\leq 0.008$ K.

(2) The error rises rapidly in the compressed liquid region below 3.5 to 4 K as the pressure rises above a few atmospheres, approaching a maximum of about 0.10 K at 50 to 100 atmospheres.

(3) A difficult region exists at pressures above about 50 atmospheres and temperatures between about 200 to 400 K, where the first deviations from the "ideal gas" eqs (23), (25), and (26) occur as a function of H or S. These deviations begin with increasing abruptness as the pressure increases, and we have not yet found a really good fit in this region. The error here can be several times the standard deviation.

(4) We have previously discussed a small residual error in McCarty's equations in the region 10 to 15 K, which shows up in this work as deviation from his predicted values by as much as 0.10 K at pressures from about 20 to about 70 atmospheres. For pressures outside of this range, the deviation drops off noticeably. It is difficult to say what the thermodynamically correct values are in this temperature region, so that an absolute error is hard to assess. It is conceivable that our equations could be accurate to within roughly their standard deviation.

## 5.0 Refrigerator Performance Survey

An important consideration in the operation of superconducting systems is the long term refrigeration performance and reliability. Statistically significant data in this area are scarce, especially on refrigerators for which long term performance data have been consistently recorded, and on refrigerators serving in less-than-ideal conditions which might typify field service.

At the inception of the ARPA contract, we began collecting documentation on refrigerator reliability from a wide number of manufacturer and user contacts throughout the USA and the world. Shortly thereafter, our group received two other assignments which, taken together, would explore this field in some depth, plus answering more specialized questions from the Naval Ordnance Laboratory and from the NBS Cryogenics for the Electrical Industry program (now defunct). As a result, only a relatively small amount of ARPA funding has gone into this type of survey, though the results remain important to the ARPA program. Both of these projects have been completed, and reports are currently in editorial process. They will be distributed to the ARPA mailing list when they become available. Also they will be presented at the Cryogenic Cooler Conference to be held at the U. S. Air Force Academy in October 1973.

The first of these studies has been done with particular reference to refrigerators for cooling infrared sensors. The approach has been to consider all factors which contribute to refrigerator system performance under field conditions, with major weight being given to the mean time between failures (MTBF), the maintainability, and the maintenance interval. The project necessarily involves a degree of subjective evaluation of the sparse data which exists. Our tentative conclusion is that with careful selection of present technology one can reasonably expect to obtain low capacity "mass purchased" (in numbers of 50 to 100 at a time) refrigerators having a MTBF on the order of

6000 hours. As the system size increases, even less data are available, but there is no reason to expect any dramatic decrease in achievable MTBF from that of the small machines.

Though this particular survey has been directed towards operation in the 60 to 90 K range, it is at the same time a significant measure of the expected performance of helium temperature refrigerators. This is because the room temperature compressor, more than any other single component, is generally the controlling element in the system reliability, although one must recognize additional problems in maintaining the helium purity in the 4 K refrigerator. Also, many of the cycles considered should work with essentially undiminished reliability down to their lower limit of about 20 K, and could thus serve in conjunction with an additional Joule-Thomson circuit to extend the lowest refrigeration temperature down to the liquid helium range.

The second project of relevance to the ARPA program has been an updating of the earlier work by Strobridge [1969] on refrigerator costs, weights, volumes, and efficiencies as a function of capacity and temperature. Though much new data have been obtained in the intervening 4 years, the earlier correlations remain essentially accurate, and no new trends are evident using these basic coordinates.

## 6.0 Program Relationships and Future Goals

The work reported here has been carried out in parallel with other Cryogenics Division projects relating to helium-cooled superconducting components. Our major activity in this particular field began in 1968 with surveys and analytical studies of various modes of helium heat transfer. Some of this heat transfer work continues to this day, but the program has steadily broadened to include system studies - the interrelationships of heat transfer mechanisms, fluid flow and stability problems, refrigeration requirements, and auxiliary pumps and equipment [Smith, 1968; Sixsmith and Giarratano, 1970; Giarratano, Arp, and Smith, 1971; Snyder, 1970; Arp, 1969, 1971; Steward and Wallace, 1971; Arp, et al., 1972; McConnell, 1973; McCarty, 1972; and Mittag, 1973]. Of partiicular note at the present are:

(1) Study of thermal stability of forced-flow helium cooling systems, with application to superconducting power lines (funded by Brookhaven National Laboratory).

(2) Studies of refrigeration requirements for superconducting power lines (funding beginning momentarily by Stanford University).

(3) Study to evaluate transient heat transfer rates, and flow system response to transient heat input (internal NBS funding).

(4) Study of helium pumps and pumping problems (funded by WPAFB, and currently by ARPA).

(5) Study of forced flow problems and heat transfer with superfluid helium (funding by AEC and ONR).

From an overview of these programs, we feel that work has progressed to the point where a major new experimental facility is called for. Using modular construction, one component of the facility would be a pumping unit, utilizing either one of our existing helium pumps, or future pumps for test. The second component would be a modular section of flow loop which could be changed from experiment to experiment to fit particular needs. The design would allow the helium in the flow loop to be controlled at any pressure and temperature of interest, including subcooled liquid, normally boiling liquid, supercritical fluid, and even boiling and subcooled superfluid ranges. Flow rate through the system would be controlled by a variable speed pump and/or appropriate valving. We are presently working out the preliminary design for such a system. It is obviously complex, but no more so than other cryogenic systems within our knowledge, and entirely within the present state of the art within our laboratory. We do not yet have funding for the project, and are restricting the work to preliminary design at this time, using WPAFB and ARPA funds.

Between now and the end of the present contract period, December 31, 1973, we plan to (1) complete the equation-of-state studies described in section 4.0 of this report, (2) complete a study of helium pump performance which has begun but is not explicitly reported here, (3) complete preliminary design on the pump-flow facility described above, and begin assembly if additional funding is obtained, and (4) complete and report upon possible Ledinegg instabilities.

## 7.0 Nomenclature and Thermodynamic Relationship

### 7.1 Nomenclature

| | | | SI Units |
|---|---|---|---|
| $a$ | = | cross-sectional area of flow channel | $m^2$ |
| $C$ | = | velocity of sound | m/s |
| $D$ | = | hydraulic diameter = $p/4a$ | m |
| $\epsilon$ | = | efficiency | |
| $G$ | = | mass flow rate/unit area = $\rho U$ | $kg/(m^2 s)$ |
| $h$ | = | heat transfer coefficient | $W/m^2 K$ |
| $H$ | = | enthalpy/unit mass | J/kg |
| $\Lambda$ | = | heat transferred into the fluid per unit length of flow channel | W/m |
| $\lambda$ | = | thermal conductivity | W/mK |
| $m$ | = | total mass flow rate = $\rho U a$ | kg/s |
| $M$ | = | Mach number = $\frac{\text{fluid velocity}}{\text{sound velocity}}$ | |
| $N$ | = | $\frac{\text{fluid velocity}}{\text{"expansion velocity"}}$; (see thermodynamics definitions) | |
| $Nu$ | = | Nusselt number = $hD/\lambda$ | |
| $p$ | = | perimeter of flow channel | m |
| $P$ | = | pressure | $N/m^2$ |
| $q$ | = | heat flux = $\Lambda p$ | $W/m^2$ |
| $\rho$ | = | density | $kg/m^3$ |
| $Re$ | = | Reynold number = $GD/\mu$ | |

| | | | SI Units |
|---|---|---|---|
| $S$ | = | entropy/unit mass | J/kg K |
| $T$ | = | temperature | K |
| $U$ | = | flow velocity (average) = $GV$ | m/s |
| $V$ | = | specific volume = $1/\rho$ | $m^3/kg$ |
| $\mu$ | = | viscosity | m·s/kg |
| $z$ | = | dimension in direction of flow | m |

## 7.2 Thermodynamic Definitions

| | | SI Units |
|---|---|---|
| $\alpha$ | $= \frac{1}{V}\left.\frac{\partial V}{\partial T}\right\|_P$ | $K^{-1}$ |
| $k$ | $= \frac{1}{\rho}\left.\frac{\partial \rho}{\partial P}\right\|_T$ | $m^2/N$ |
| $x$ | $= \frac{1}{V}\left.\frac{\partial V}{\partial H}\right\|_P$ | $kg/J$ |
| $\psi$ | $= \left.\frac{\partial T}{\partial P}\right\|_H = (\alpha T - 1)/(\rho C_P)$ | $m^2 k/N$ |
| $\theta$ | $= \frac{1}{\rho}\left.\frac{\partial \rho}{\partial P}\right\|_H = k - \alpha\psi$ | $m^2/N$ |
| $\omega$ | $= (C_P/\alpha)^{1/2}$, "expansion velocity" | $m/s$ |
| $c$ | $= (\gamma/\rho k)^{1/2}$, velocity of sound | $m/s$ |
| $\gamma$ | $= C_P/C_V = 1 + \alpha T\left(\frac{c^2}{\omega^2}\right)$ | — |
| $\rho\theta$ | $= \frac{1}{\omega^2} + \frac{1}{c^2}$ | $s^2/m^2$ |

7.3 Typical Values in Liquid Helium Range

| | Subcooled Liquid | Vapor (ideal gas) | Near-Critical Fluid |
|---|---|---|---|
| $\alpha T = \frac{T}{V}\frac{\partial V}{\partial T}\Big\|_P \approx$ | 0.2 | 1.0 | 20. |
| $Pk = \frac{P}{\rho}\frac{\partial \rho}{\partial P}\Big\|_T \approx$ | 0.03 | 1.0 | 10. |

$\omega \approx C \approx$ 150 meters per second

7.4 The Temperature Change of a Real Fluid Through a Pump or Engine

The input mechanical work per unit mass flow, dW, through a pump or engine is equal to the increase in the stagnation enthalpy $(H + 1/2\ U^2)$ from inlet to outlet. Neglecting the kinetic energy term, this can be written

$$dW = dH = TdS + VdP\ .$$

In this convention dW, dH, and dP are positive for pumps and negative for engines. On the other hand, the entropy change dS from inlet to outlet will always be $\geq 0$, by the Second Law. The input work to an ideal (isentropic) device operating over the same pressure range dP will be

$$dW_i = dH_i = VdP$$

For a pump, $dW > dW_i$, and the efficiency $\epsilon_P$ is defined

$$\epsilon_P = \frac{dW_i}{dW}.$$

By simple substitution the entropy increase as a function of the pump efficiency is then found to be

$$dS = \left(\frac{1}{\epsilon_P} - 1\right) \frac{V dP}{T} .$$

For an engine, $|dW_i| > |dW|$, and the efficiency is defined

$$\epsilon_e = \frac{|dW|}{|dW_i|}$$

so that the entropy increase is

$$dS = (1 - \epsilon_e) \frac{V}{T} (-dP) .$$

In either case, the temperature increase through the device, from inlet to outlet, is given by

$$dT = \left.\frac{\partial T}{\partial P}\right|_S dP + \left.\frac{\partial T}{\partial S}\right|_P dS$$

where the first term can be related to real fluid properties in an ideal (isentropic) process, and the second term can be related to irreversibilities in the process itself. Using straightforward thermodynamic identities, this last equation can be written

$$dT = \left(\psi + \frac{V}{C_P}\right) dP + \frac{T}{C_P} dS .$$

Substituting dS ($\epsilon p$) for a pump, we find

$$\left.\frac{dT}{dP}\right|_{PUMP} = \psi + \frac{1}{\epsilon \rho C_P}$$

and for an engine

$$\left.\frac{dT}{dP}\right|_{ENGINE} = \psi + \frac{\epsilon}{\rho C_P} .$$

A real pump or engine may operate over a large $\Delta P$ such that these differential equations are inadequate as they stand. They can be integrated between required inlet and outlet pressures (or temperatures), but to our initial surprise we found that the integrated results correspond to overall efficiencies which differ from the given efficiency by up to 10 or 20%, for typical refrigeration calculations. After some thought, we deduced that the discrepancy occurs because the entropy corresponding to the isentropic compression $dH_i$ changes implicitly at each integration step, whereas the entropy used to check the integrated results always equals that at the inlet to the device. Nevertheless, the equations provide a useful semi-quantitative estimate of $\Delta T / \Delta P$ in a real device.

## 8.0 Acknowledgements

The research output of the Cryogenics Division depends strongly upon informal and cooperative input from the many employees whose expertise overlaps the project at hand. Michael Jones and co-workers have been a valuable source of ideas and information on the hydrodynamics of helium flow. Robert McCarty has given generously of advice and review on the development of the helium state equations. Jesse Hord has provided valuable input to the systems concepts within the program. Roland Voth and Richard Strobridge have done the survey work summarized in section 5.0. Neil Houbolt has been a most patient and persistent programmer for many of the computer analyses.

## 9.0 References


Arp, V., Heat transport through He II, Cryogenics 10, 96 (1970).

Arp, V., Forced-flow, single phase helium cooling systems, Book, Advances in Cryogenic Engineering 17, p. 342 (1972).

Bald, W. B., Supercritical helium cooling of hollow superconductors; Part II, Thermal instabilities, Brookhaven National Laboratory Note 15805 (1970).

Bird, R. B., Stewart, W. E., and Lightfoot, E. N., Transport Phenomena (John Wiley and Sons, New York, N. Y., 1960).

Chivers, T. C., and Mitchell, L. A., On the limiting velocity through parallel bore tubes, J. Phys. D: Appl. Phys. 4, 1069 (1971).

Dean, J. W., and Mann, D. B., The Joule-Thomson Process in Cryogenic Engineering, Nat. Bur. Stand. (U.S.), Tech. Note 227 (1965).

Giarratano, P. J., Arp, V., and Smith, R. V., Forced convection heat transfer to supercritical helium, Cryogenics 11, 385 (1971).

Greene, W. J., and Saibel, E., Stability of internally-cooled superconductors, Book, Advances in Cryogenic Engineering 14, p. 138 (1968).

Krasiakova, I. I., and Glusker, B. N., Energomashinostroenie 9, 18 (1965).

Ledinegg, M., Instability of flow during natural and forced circulation, Die Warme 61, No. 8 (1938); AEC translation 1861 (1954).

Linhardt, H. D., Cryogenic turboexpanders, LNG/Cryogenics 1, No. 7 (1973).

McCarty, R. D., Thermophysical properties of helium-4 from 2 to 1500 K with pressures to 1000 atmospheres, Nat. Bur. Stand. (U.S.) Tech. Note 631 (1972).

McCarty, R. D., Thermophysical properties of helium from 2 to 1500 K at pressures to $1 \times 10^8$ pascals, To be published (1973).

McConnell, P. M., Liquid helium pumps, Nat. Bur. Stand. (U. S.) Interagency Report 73-316 (1973).

Mittag, K., Kapitza conductance and thermal conductivity of copper, niobium, and aluminum in the range 1.3 to 2.1 K, Cryogenics 13, 94 (1973).

Semenkover, I. E., Energomashinostroenie 3, 16 (1964).

Sixsmith, H., and Giarratano, P. J., A miniature centrifugal pump, Rev. Sci. Inst. 41, 1570 (1970).

Smith, R. V., Review of heat transfer to helium I, Cryogenics 9, No. 11 (1968).

Snyder, N. S., Thermal conductance at the interface of and helium II, Nat. Bur. Stand. (U. S.) Tech. Note 385 (1969).

Steward, W. G., and Wallace, G. H., Helium viscosity measurements - 4 to 20 K, 0 to 10 MN/$m^2$, Nat. Bur. Stand. Report (unpublished) (1971).

Strobridge, T. R., Private communication (1973).

Strobridge, T. R., Refrigeration for superconducting and cryogenic systems, IEEE Trans. on Nuclear Science NS-16 (1969).

Zuber, N., An analysis of thermally induced flow oscillations in the near-critical and super-critical thermodynamic region, NASA Report NAS8-11422, DDC accession number N67-13534 (1966).

FORM NBS-114A (1-71)

| U.S. DEPT. OF COMM. BIBLIOGRAPHIC DATA SHEET | 1. PUBLICATION OR REPORT NO. NBSIR 73-331 | 2. Gov't Accession No. | 3. Recipient's Accession No. |
|---|---|---|---|

4. TITLE AND SUBTITLE

REFRIGERATION OF SUPERCONDUCTING ROTATING MACHINERY

5. Publication Date: June 1973

6. Performing Organization Code

7. AUTHOR(S)
Vincent D. Arp

8. Performing Organization

9. PERFORMING ORGANIZATION NAME AND ADDRESS

NATIONAL BUREAU OF STANDARDS, Boulder Labs.
DEPARTMENT OF COMMERCE
Boulder, Colorado 80302

10. Project/Task/Work Unit No. 2750452

11. Contract/Grant No. 2186

12. Sponsoring Organization Name and Address

Defense Advanced Research Projects Agency
1400 Wilson Boulevard
Arlington, Virginia 22209

13. Type of Report & Period Covered

14. Sponsoring Agency Code

15. SUPPLEMENTARY NOTES

16. ABSTRACT (A 200-word or less factual summary of most significant information. If document includes a significant bibliography or literature survey, mention it here.)

Recent work at the NBS Cryogenics Division in three areas related to helium refrigeration is summarized: (1) Analysis is given of a possible high pressure refrigeration cycle which offers in principle a reduced component size, but which turns out to be impractical because of expansion engine inefficiencies. (2) Exact equations for flow of a real fluid are derived and applied to problems of fluid flow near the critical point, as may occur with some helium-cooled superconducting systems, and (3) Three new equations of state for helium are given, each using different state variables, to eliminate the need for iterative techniques in helium refrigeration cycle and fluid flow analysis.

17. KEY WORDS (Alphabetical order, separated by semicolons)

Equation of state; helium; hydrodynamics; near-critical flow; refrigeration; superconductors; thermodynamics.

18. AVAILABILITY STATEMENT

[X] UNLIMITED.

[ ] FOR OFFICIAL DISTRIBUTION. DO NOT RELEASE TO NTIS.

| 19. SECURITY CLASS (THIS REPORT) | 21. NO. OF PAGES |
|---|---|
| UNCLASSIFIED | |
| 20. SECURITY CLASS (THIS PAGE) | 22. Price |
| UNCLASSIFIED | |